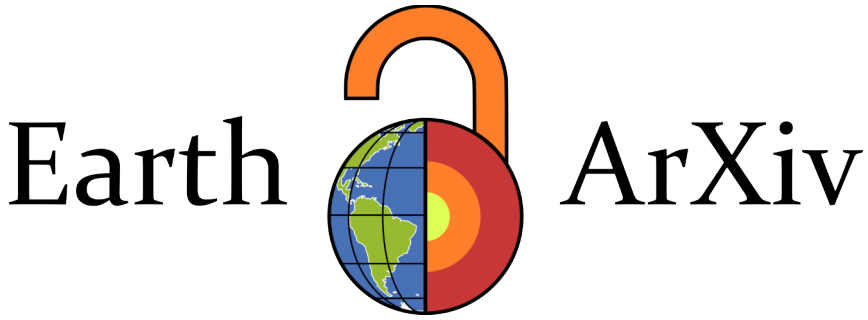

# EXPLORATION OF WATER RESOURCES MANAGEMENT DECISION SUPPORT POTENTIAL IN DATA SCARCE WATERSHEDS AND ASSOCIATED DATA POLICY NEEDS

**Victoria M. Garibay[1,2], Margaret W. Gitau[1], Daniel Moriasi[3]**

[1] Department of Agricultural & Biological Engineering, Purdue University, West Lafayette, IN, USA

[2] Informatics Institute, University of Amsterdam, Amsterdam, NH, Netherlands

[3] USDA ARS Grazinglands Research Laboratory, El Reno, OK, USA

## Abstract

Insufficient data access presents major challenges to scientific assessment of water resources, development of management plans, and attainment of water security. Hydrologic models are widely applied in the advisement of pollution, drought, and flood mitigation strategies; their accuracy relies on data used in setup and calibration. A case study of Sasumua River Watershed in Kenya illustrates compromises in certainty that must be made when conducting research and developing hydrologic models under unideal data conditions. Current results predict a substantial increase in streamflow within 50 years and recommend a multi-faceted approach to agricultural pollutant reduction. Direct experience from the case study reiterates the importance of organized data collection and dissemination for metrics of concern to improve future efforts in data-scarce regions.

Keywords: water resources, water security, data policy, data scarce, modeling, decision making, climate, CMIP6, SWAT

## 1 Introduction

High quality data and hydrologic model outputs present tremendous opportunities to inform decisions pertaining to water supply, quality, and climate extremes. This advantage has been realized in several studies addressing topics including efficient implementation of management practices (Mwangi et al., 2015; Gitau et al., 2006), flood risk management (Khaing et al., 2019;

Hall et al., 2003), and optimization of water resource allocation (Mirdashtvan et al., 2021) to name a few. The functionality of hydrologic models is inherently dependent upon climate and water data, which makes analyses for data-scarce regions extremely challenging.

Some techniques that have been used to overcome data limitations include using downscaled global climate datasets and using calibration parameters from a previously calibrated model in proximate or physically similar locations (Alipour & Kibler, 2019; Dinku et al., 2011; Gitau & Chaubey, 2010). Despite these capacity development efforts, data scarcity and unavailability remain an acknowledged stumbling block to studies aiming to address key issues surrounding climate and hydrology. Kwakye & Bárdossy (2020) exemplify how it impacts the complexity of models that can be applied in a region, with the level of detail required and provided by conceptual or process-based modeling sometimes being sacrificed in favor of the simplicity of empirical modelling. As stated by Khaing et al. (2019), hydrometeorological data scarcity results in the unavailability of reliable flood maps and information for urban planning, consequently causing preventable damage to vulnerable populations. For studies which rely on remotely sensed measurements (e.g., Penatti et al., 2015, Alemayehu et al., 2016), lack of ground measurements, temporal or spatial, still limits attempts to calibrate and validate models (Grey et al., 2013); as mentioned by Dinku et al. (2011), even in a case where there may be a sufficient quantity of measurement stations, the stations are not always well distributed, often to the detriment of rural communities. Without access to data resources that are essential to the creation of high-quality models, these tools cannot be utilized to their full potential. Increasingly pronounced climate variability has made it crucial to devise data-driven plans for the management of water resources and the protection of those who rely on them. Given that the need for coordinated data collection efforts is increasing in response to integration of water resources management across disciplines (WMO, 2020), data collection and dissemination policy reform is now imperative. Some of the missing elements outlined by Grey et al. (2013) to effectively assess hydrologic threats are a consensus on data architecture, including language, metrics, and standards; they elaborate that achieving global agreement on these will aid interdisciplinary researchers in communication in the face of complex challenges. Overpeck et al. and Grey et al. both emphasize the role of technological progress as a solution to data scarcity, both in the form of crowd-based measurements and remote sensing. As these

advancements begin to gain traction and usage, there is a unique opportunity to lay a foundation of standards and practices for their development.

When conducting studies in a data-rich environment, it is possible to report with more certainty the results of an analysis including approximations of pollutant concentrations or stream flow rates rather than relying on relative change metrics. Examples of studies made possible by data-rich resources include prediction of phosphorous loading from agricultural anthropogenic sources, estimating water quality and discharge response to land use change, performance assessment of best management practices, and quantification of discharge response to groundwater abstractions (Sinclair et al., 2014; Noteboom et al., 2021; Sholichin & Qadri, 2020; Affessa et al., 2022; Liu et al., 2020; Chaubey et al., 2010). While generalized information can be garnered from studies under sparse data conditions, the resolution and quality of input data have an important impact on model results (Smit & van Tol, 2022; Rocha et al., 2020; Penatti et al., 2015).

This study demonstrates use of data for water resources management decision-making in the Sasumua River Watershed in Kenya. Specifically, it provides a practical case study which 1) shows how data can be translated into management decisions and 2) forms a basis for recommendations on how to improve data availability and access for decision-making and management in the future. The case study serves as an illustration of the challenges and limitations in applying data-driven techniques given the current state of regional data resources. In this light, recommendations were made for the path forward for data policy so that sufficient data resources can be established, adding precision and value to studies upon which sound management decisions can be founded. The case study was conducted using readily available resources in a consciously transparent manner, enabling the definition of challenges specific to the study area and the development of strategies to improve the quality of this type of study in the future as a result of targeted data acquisition and increased accessibility.

## 2 Case Study Description

### 2.1 Study Site Overview

The area selected for a demonstrative case study was the Sasumua River Watershed, located in Nyandarua County and within Kenya's Tana River Basin (Fig. 1). This headwaters watershed is of particular significance as it is responsible for 15 to 20% of the water supply for Nairobi (Mwangi et al., 2015). The Sasumua Dam, Kiburu Dam and Chania Dam as well as two diversions referred to as the Chania Tunnel and Kiburu Diversion were established to stabilize levels in the Sasumua Reservoir and help in meeting this demand (Dixon & Berry, 1970). The catchment area covers approximately 136 $km^2$, and elevation within ranges from 2250 to 3880 m; it is primarily comprised of farmland as well as forested areas overlapping the southwestern portion of the Aberdare Mountain Range (Fig. 1b; Nduhiu et al., 2016), which forms part of the eastern rim of the Great Rift Valley. On an annual basis, the watershed receives rainfall during the long and short rainy seasons—consistent with the region—with an average total rainfall of 1,000 to 1,600 mm (Gathenya et al., 2009, as cited in Mwangi et al., 2015). The period of March through June coincides with the long rains season, and October through December comprises the short rains season (Nakaegawa et al., 2012). Due to the proximity of farmland to the river and reservoir as well as the steep slopes surrounding them, sediment and nutrient loadings to the reservoir are current water quality concerns. Soil erosion is a particular issue for uncultivated grasslands in the region (Kyei, 2020). The soil profiles represented in the watershed are Andosols joined by a Planosol (KE134-1-58) and a Phaeozem (KE134-3-48) distributed as shown in Figure 1c.

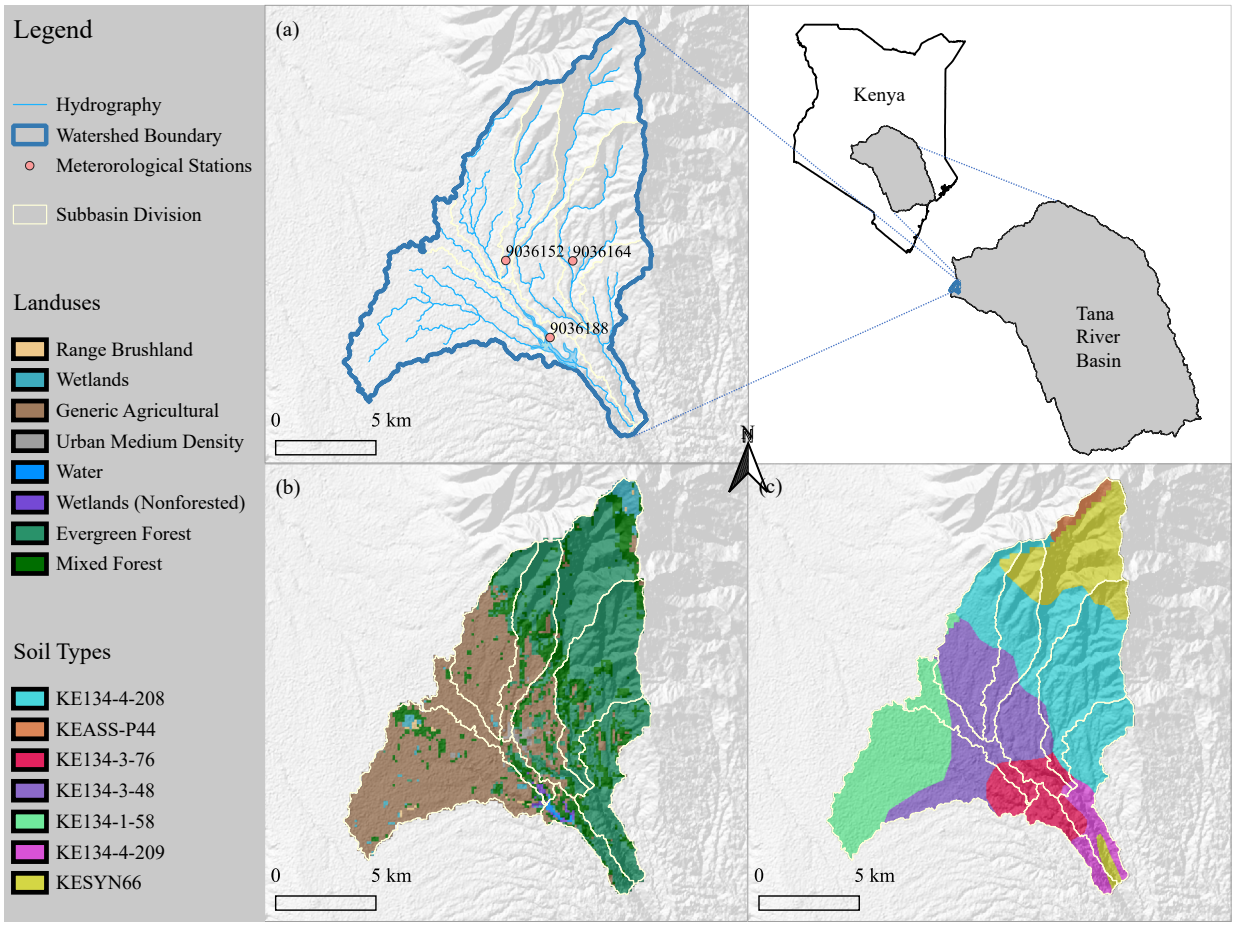


**Figure 1** Map of Sasumua River Watershed and a) Sasumua Reservoir and nearby meteorological stations, b) landuse adapted from Copernicus 2015 product, and c) soil types adapted from SOTER_UT and KENSOTER v2 products. Data from b and c were used in hydrologic modelling activities.

## 2.2 Methodology

A modelling approach was taken for this study using the Soil and Water Assessment Tool (SWAT, Arnold et al., 1998)—a distributed parameter model originally developed to assist evaluation of management practices and other changes through the continuous simulation of hydrologic processes for large river basins. The model has since been applied extensively around the world (Bailey et al., 2020) including the Sasumua River Watershed (Mwangi et al., 2015; Nduhiu et al., 2016). A more recent, modified version of SWAT with restructured code and inputs, SWAT+, was developed to more flexibly accommodate the spatial representation of basin processes (Bieger et al., 2017). This new version was used in the case study.

The unavailability of data and consciousness of data scarcity in the East African region shaped the approach to developing the watershed model. SWAT+ requires information from climate, elevation, land use, and soils datasets for basic functionality. Baseline data used in this study is discussed in ensuing subsections. Model parameters can subsequently be calibrated to accommodate local conditions using hard data from streamflow gauges and other point observations and soft data such as a known water balance composition or literature-based component estimates. It is recommended to use both types of data when calibrating a SWAT+ model (Seibert & McDonnel, 2002). Due to unavailability of standard streamflow and water quality data for use with model calibration and validation, a soft data calibration approach was used in this study. The baseline watershed model was then used to evaluate the effects of different management practices and climate change trajectories on the watershed.

### 2.3 Data Development

A collection of datasets for elevation, land use, soil, and climate data were accumulated and pieced together from relevant agencies and portals for use as model inputs, as described in ensuing subsections. Special attention was placed on replicability, guided by relevant documentation (Saraswat et al., 2015) such that elements of the study can be revisited and improved as the regional data situation evolves. In line with FAIR Guiding Principles (Wilkinson et al., 2016), the use of openly accessible data resources was prioritized in building the model with the option of sourcing and/or purchasing data being used when open access options had been exhausted or had not yielded suitable results. Data inputs used in this study were obtained and developed as detailed in Appendix I (summarized in Table 1):

**Table 1** Summary of data inputs used in development of the Sasumua River Watershed SWAT model.

| Data Type | Source† | Description | Current Availability |
|---|---|---|---|
| Topography | NASA JPL, 2013 (SRTM) | Digital elevation model raster | Freely Available for Download |
| Soils | Dijkshoorn et al., 2011 (SOTER_UT); Batjes & Gicheru, 2004 (KENSOTER); Hengl et al., 2017 (ISRIC SoilGrids250m) | Vectorized map and corresponding database of soil profile information | Freely Available for Download |
| Land Use | Buchhorn et al., 2020 (Copernicus) | Remotely sensed land use/ land cover raster | Freely Available for Download |

| | | | |
|---|---|---|---|
| Climate | Saha et al., 2010 (CFSR); Saha et al., 2011 (CFSRv2) | Daily precipitation totals and temperature extremes | Freely Available for Download |
| Climate Projections | O'Neill et al., 2016 (CMIP6) | Daily precipitation totals and temperature extremes for future climate scenarios | Freely Available for Download |
| Agronomic Practices | County Government of Nyandarua, 2018; Jaetzold et al., 2006 | Information on crops, growing seasons, and operations. | Freely Available for Download |
| Agronomic Inputs | Oseko & Dienya 2015; Jaetzold et al., 2006 | Information on chemical fertilizer and manure inputs | Freely Available for Download |
| Streamflow | WRA | Daily streamflow records | Rating Curve Unavailable Upon Request |
| Water Quality | WRA | | Unavailable Upon Request |

†NASA JPL: National Aeronautics and Space Administration Jet Propulsion Laboratory; SRTM Shuttle Radar Topography Mission; SOTER_UT: Upper Tana Soil and Terrain; KENSOTER: Kenya Soil and Terrain; CFSR: Climate Forecast System Reanalysis; CMIP6: Coupled Model Intercomparison Project Phase 6; WRA: Kenya Water Resources Authority.

## 2.4 Model Development, Calibration, and Validation

A model of the Sasumua River Watershed was established in SWAT+. Appendix I contains technical details and extended information on development of the model which featured 8 subbasins and 1,167 HRUs. Daily data on flowrates for the Kiburu or Chania diversions were not available, therefore, these features were modelled as a simplified 90% diversion of flow from the channel at the diversion entrance to the exit point.

The calibration period consisted of 2011-2015, with a 5-year warm up, and the validation period spanned 2016-2020. A local sensitivity analysis indicated that surface runoff (SR) and evapotranspiration (ET) were less sensitive to the parameters petco, flo_min, and abf_lte (Table S6). Saltelli first-order and Jansen total-order sensitivity analysis indicated important effects for cn3_swf, epco, latq_co, esco and cn2, although sensitivities did not converge for all parameters (Fig. S6, Table S7).

The target composition values for SR and ET were 14% and 75% of annual rainfall for the calibration period, respectively, based on the corresponding ranges of 12-16% and 65-90% calculated and modelled in studies by Archer (1996), Hunink, et al. (2011), and Mwangi, et al. (2015). The highest mean percentage of ET achieved over the calibration period in the entire testing space was 44.1%, and mean annual percentage ET could not be raised substantially without raising mean annual percentage SR beyond the desired range.

## 2.5 Scenario Definition

A field visit to WRA in Nairobi and the watershed site was conducted to ground truth data on land cover and agricultural practices and verify the location of known points within the case study area.

Another primary function of the trip was to assess the types of outputs and scenarios that would be of greatest value or interest to stakeholders. One expression from the WRA—the agency charged with regulating use and management of Kenya's water resources—was a desire for more information on groundwater responses in the region of the case study. Meetings with representatives of the Upper Tana-Nairobi Water Fund (UTNWF)—initially founded by The Nature Conservancy to protect upstream water resources, now run locally with similar goals—revealed interest in modelling the effects of different practices with planned or ongoing implementation in the watershed; these included runoff collection in constructed, lined ponds, level field diversions for water storage, Napier edge-of-field grass strips, and riparian buffer zones. The following management scenarios, outlined in Table 2, were designed to fit the needs of the watershed with consideration to the input received from WRA, UTNWF, and other stakeholders.

The first management scenario modelled the establishment of 100-m riparian buffers along streams, the second addressed the application of vegetative contour strips in agricultural areas, and the third scenario was representative of terracing in agricultural areas. Scenario 4 was the implementation of level field diversions and Scenario 5 modelled the adoption of agricultural water harvesting pond systems. Scenarios 1-5 applied a single practice while Scenario 6 represented the combination of several of these practices together, namely riparian buffers, filter strips, terracing, and water harvesting ponds. Adjustments to the universal soil loss equation (USLE) P factor were applied to the calibrated model and Scenarios 3, 4, and 6 using the land use management feature in SWAT+ Editor. Field border filter strips were applied for Scenarios 2 and 6 also using the land use management feature in SWAT+ Editor. For design purposes in Scenarios 5 and 6, generic agricultural water harvesting pond systems consisted of 3x2x2 m pits lined with plastic. Similar to methods used in Ghimire and Johnston (2013), floor division of the area of each agricultural HRU by an average agricultural land holding size of 1.73 acres (County

Government of Nyandarua, 2018) was used to approximate the number of runoff harvesting ponds. For each subbasin, ponds were aggregated into a single pond of equivalent volume and surface area located at the points indicated in Figure 2. Due to a lack of information on quantity and timing of irrigation operations, and given that most agriculture in the watershed is rainfed, scenarios related to irrigation were not modelled in this study.

Precipitation and temperature data for four future climate scenarios—SSP1/RCP2.6 (sustainable), SSP2/RCP4.5 (mixed), SSP3/RCP7.0 (environmentally unconcerned), and SSP5/RCP8.5 (fossil-fuel-driven)—was retrieved from the Coupled Model Intercomparison Project Phase 6 (CMIP6, O'Neill et al., 2016) for use as climate inputs in the calibrated SWAT+ project to predict the effects of climate change on discharge into the Sasumua Reservoir considering the periods: 2011-2020 (baseline) and successive twenty-year periods in the near, middle, and distant future (2031-2050, 2051-2070, and 2071-2090, respectively). Datasets from seven separate models were considered for a total of 28 SWAT model outputs.

**Table 2** Baseline model management practice and changes made to the baseline model by scenario.

| **Management Scenario** | **Modifications** |
|---|---|
| Baseline | Cross slope tillage implemented on agricultural land using SWAT+ Editor (P Factor = 0.75). |
| 1 Riparian Buffers (100m) | The Copernicus land cover raster was modified to include a 100 m buffer of rangeland around the stream network, and the baseline model was redeveloped and run using this updated land cover layer. |
| 2 Filter Strips | Field Border filter strips were implemented on agricultural land using SWAT+ Editor. |
| 3 Terracing | Contoured terraces on 3-8% slopes with sod outlets implemented on agricultural land using SWAT+ Editor (P Factor = 0.5). |
| 4 Field Diversions | Field diversion terraces at 40 m intervals on 3-8% slopes implemented on agricultural land using SWAT+ Editor by creating a new conservation practice based on Yang, et al. (2009) (P=0.17). |
| 5 Agricultural Water Harvesting Ponds | Ponds with a volume and surface area equivalent to the sum of runoff harvesting system volumes estimated for agricultural HRUs were placed within each subbasin, and the baseline model was redeveloped and run using this updated inlet/outlet layer. |
| 6 Combined Application of Riparian Buffers (100 m), Filter Strips, Terracing, & Agricultural Water Harvesting Ponds | Modifications for Scenarios 1, 2, 3, and 5 above applied to a single model. |

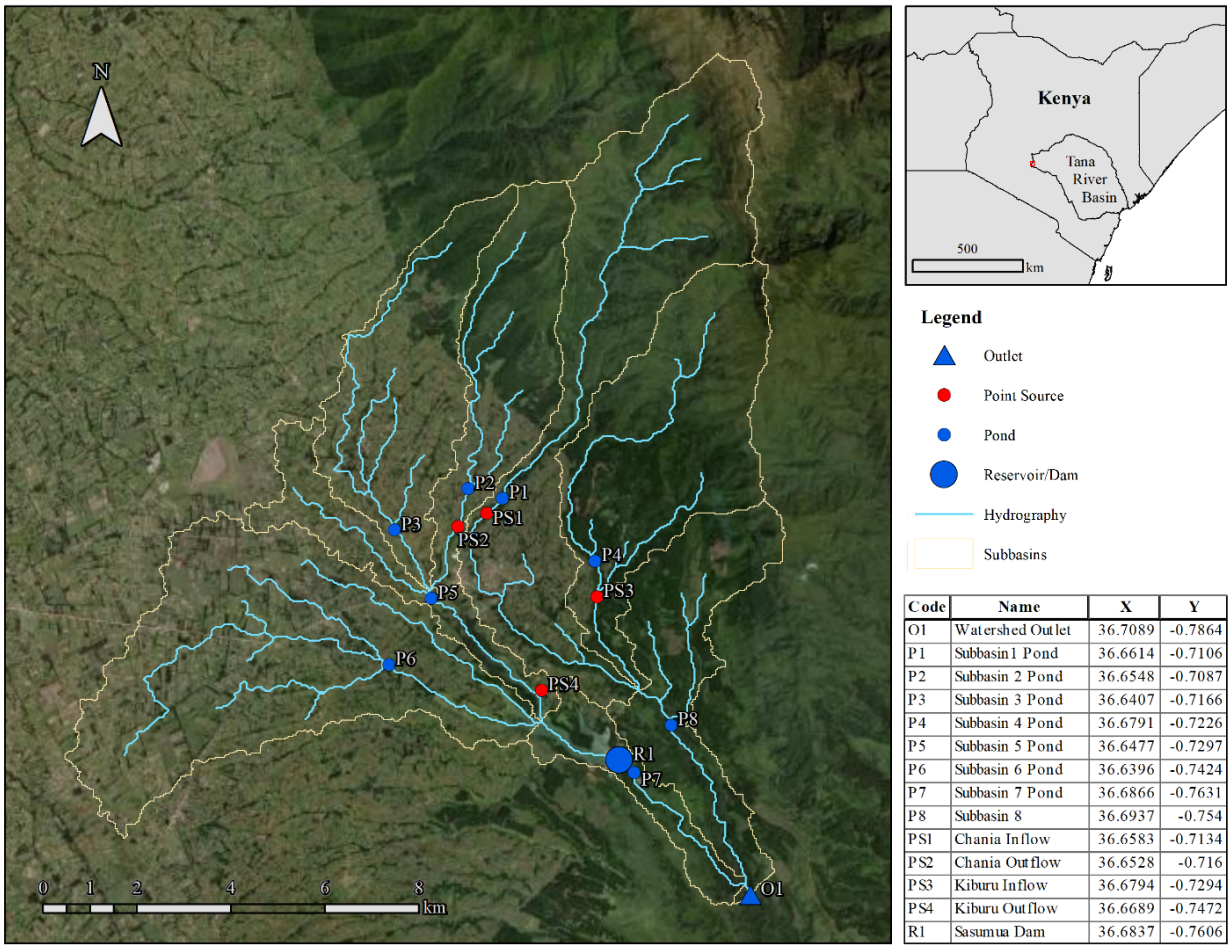


| Code | Name | X | Y |
|---|---|---|---|
| O1 | Watershed Outlet | 36.7089 | -0.7864 |
| P1 | Subbasin1 Pond | 36.6614 | -0.7106 |
| P2 | Subbasin 2 Pond | 36.6548 | -0.7087 |
| P3 | Subbasin 3 Pond | 36.6407 | -0.7166 |
| P4 | Subbasin 4 Pond | 36.6791 | -0.7226 |
| P5 | Subbasin 5 Pond | 36.6477 | -0.7297 |
| P6 | Subbasin 6 Pond | 36.6396 | -0.7424 |
| P7 | Subbasin 7 Pond | 36.6866 | -0.7631 |
| P8 | Subbasin 8 | 36.6937 | -0.754 |
| PS1 | Chania Inflow | 36.6583 | -0.7134 |
| PS2 | Chania Outflow | 36.6528 | -0.716 |
| PS3 | Kiburu Inflow | 36.6794 | -0.7294 |
| PS4 | Kiburu Outflow | 36.6689 | -0.7472 |
| R1 | Sasumua Dam | 36.6837 | -0.7606 |

**Figure 2** Map of Sasumua River Watershed and relevant points used in hydrologic modelling activities.

## 3 Results and Discussion

The Sasumua River Watershed case study encompassed the calibration and validation of a SWAT+ model and the practical evaluation of the outputs resulting from different scenarios tested. Experiences during the process were used to support commentary on what actions should be taken on a greater scale to improve the availability of data resources for future modelling efforts.

### 3.1 Case Study Results

Using the calibrated model, the mean annual percentage compositions for SR and ET were 15% and 43% of precipitation for the calibration period and 20% and 37% for the validation period, respectively. Results achieved for SR for these periods were within a satisfactory range compared to literature. However, calibration of the model within reasonable parameter ranges consistently underestimated the ET component of the water balance when compared as a percentage to values from literature. As the model results form the basis of recommendations for action, it is important to note this discrepancy. While variations in ET calculations between SWAT+ versions have been noted by user groups, more work is needed to pinpoint the cause. Annual values for sediment yield (0.04 tons/ha for the calibration period and 0.07 tons/ha for the validation period) were well within the range of literature suggested values (0-10 tons/ha). Since the average annual sediment yield values were consistent with the literature, no calibration of transport-related parameters was deemed necessary.

#### 3.1.1 Management Scenario Results

Listed in Table 3 are the mean annual sediment, organic nitrogen, and organic phosphorous yields and $NO_3$ in runoff for the entire watershed for the 2011-2020 period. The effects of each management scenario varied across these dimensions, with filter strips (Scenario 2) having the best efficacy for a single measure at reducing losses and Scenario 6, with multiple practices combined, resulting in the greatest reduction of losses. Scenarios 1 and 5, representing rangeland buffers and agricultural water harvesting ponds led to loss increases, most notably for $NO_3$ in runoff. However, these effects were mitigated when combined with filter strips and terracing for Scenario 6. A comparison by subbasin highlighted which areas were more susceptible to sediment loss in the baseline model (Fig. 9a). The sediment losses for each of the scenarios were

also compared at the subbasin level to the baseline loss (Fig. 9b-g). In almost all cases sediment yield was considerably reduced with exceptions being for the near-zero percent change of implementing Scenario 5 and the increase in sediment loss for the south-easternmost subbasin in Scenario 1. This particular subbasin was primarily forested in the baseline scenario, thus the application of a uniform rangeland buffer to some areas which were previously forested implied a land use change resulting in the visualized 13% increase in loss. The importance of maintaining existing forest buffers should be acknowledged as Figure 1b indicates that agricultural land use is encroaching on this subbasin and the subbasin to its north. Subbasin responses for organic N and P followed a similar pattern to sediment (Figs. S9 & S10).

**Table 3** Comparison of sediment yield, total nitrogen loss, total phosphorous loss, nitrate in runoff, surface runoff, and evapotranspiration for the watershed and inflow to the Sasumua Reservoir relative to baseline results.

| | | Percent Change (%) | | | | | |
|---|---|---|---|---|---|---|---|
| | **Baseline** | **Scenario 1** | **Scenario 2** | **Scenario 3** | **Scenario 4** | **Scenario 5** | **Scenario 6** |
| Sediment | 0.055 ton/ha | -22.9 | -30.0 | -10.2 | -23.3 | 0.2 | -46.9 |
| Organic N | 0.033 kg/ha | -14.8 | -11.7 | -4.6 | -11.4 | 0.9 | -26.8 |
| Organic P | 0.002 kg/ha | -5.3 | -5.3 | -5.3 | -5.3 | 0 | -26.3 |
| Runoff $NO_3$ | 0.116 kg/ha | 14.3 | -70.1 | 0 | 0 | 40.4 | -73.5 |
| Surface Runoff | 291 mm | 8.4 | 0 | 0 | 0 | 0.1 | 8.4 |
| Evapotranspiration | 616 mm | -4.6 | 0 | 0 | 0 | -0.1 | -4.6 |
| Reservoir Inflow | $93.8 \times 10^6$ $m^3/s$ | 4.6 | 0 | 0 | 0 | 0.7 | 5.3 |

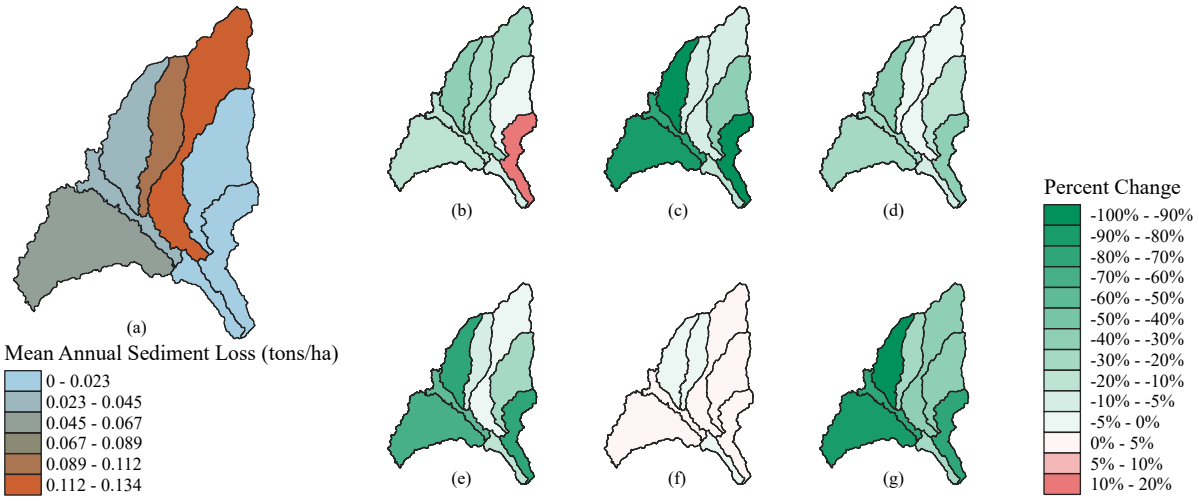


**Figure 3** Map of sediment loss by subbasin for: a) baseline; and scenarios b) 1-Riparian Buffers, c) 2-Filter Strips, d) 3-Terracing, e) 4-Field Diversions, f) 5-Agricultural Water Harvesting Ponds, and g) 6-Combined Application of 1, 2, 3, and 5. All scenario percent changes are relative to baseline. Reductions in losses are signified by a negative percent change.

### 3.1.2 Climate Change Impacts

A summary of the results from running the calibrated model with the 28 CMIP6 model outputs is shown as a series of boxplots representing the mean annual flow into the Sasumua Reservoir normalized on the basis of the median value for each of the four climate scenarios for the first twenty-year period (Fig. 4). While there is little change in SSP1/RCP2.6, mean streamflow is generally projected to increase over time with the most extreme difference between the first and last period occurring under SSP5/RCP8.5, for which flows may nearly triple. The means for less extreme climate scenarios, SSP2/RCP4.5 and SSP3/RCP7.0, more than double over the same period. This is most likely driven by the increases in precipitation for the short rains season, a projected trend also observed in literature (Cook et al., 2020). Of the seven models considered, INM-CM4.8 was responsible for all outliers and the maximum value for each climate scenario for each period (Fig. 4). In Appendix II, the results for SSP2/RCP4.5 were plotted in further detail to provide a snapshot of projected changes in monthly and seasonal flows and map subbasin-level differences in SR and ET within and across periods.

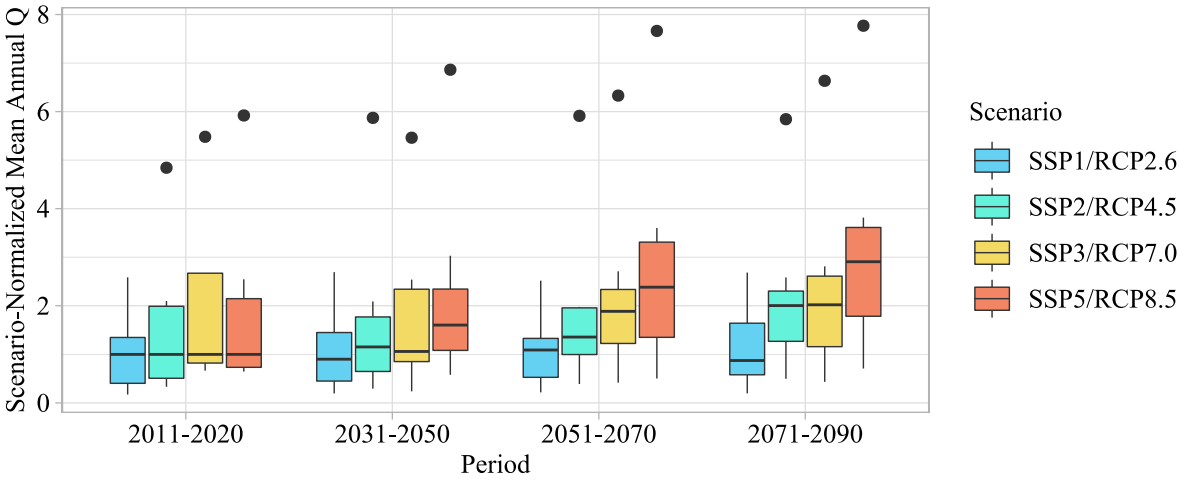


**Figure 4** Boxplots for mean annual discharge into the Sasumua Reservoir for the periods 2011-2020 (baseline), 2031-2050, 2051-2070, and 2071-2090 under SSP1/RCP2.6, SSP2/RCP4.5, SSP3/RCP7.0, and SSP5/RCP8.5 using outputs from seven CMIP6 models. Average annual flows were normalized using the median value for the first period of each climate scenario. Points represent statistical outliers and are not considered in the formation of the boxplots.

### 3.2 Study Insights

With assistance from the WRA, limited precipitation data from local stations and daily stream gauge records were procured. Unfortunately, the precipitation records were on a monthly basis, not daily, and as such could not be used in the model directly or as a guide for downscaling the climate datasets used. Similarly, the stream gauge data obtained, while at a daily timescale, was reported in height (m) and, in the absence of a stream rating curve, could not be turned into a meaningful flow rate. Literature suggests that, at some point in history, records were collected locally for meteorology, streamflow, and sedimentation (Mwangi et.al, 2015; Nduhiu et al., 2016). It is unclear why those particular datasets could not be traced and were no longer available by request. Overall, the data conditions under which the case study was performed were not ideal. There was no observed daily meteorological data, only generalized sediment data, and no nutrient, inorganic chemical, or biological component data found representative of the study area. There was very limited recent information available on measurements or studies pertaining to water quality for the watershed. Most data ranges were estimated using graphics from literature dating back a decade or more, which was focused on the Tana River Basin at large. Since the calibration and validation periods span 2011-2020, the timeliness was not

extremely discordant. However, this is something that will need to be taken into consideration for future studies.

Unfortunately, this type of experience is not uncommon in areas that can be termed as data scarce. The process of procuring data for this project was a prime example of the complexity of availability issues for data related to water resources management in the region. In many cases, the necessary systems have not yet been established to make data accessible for public research (Garibay et al., 2022). In other cases, data has been collected piecemeal through different research projects and is not being aggregated and curated in a single research database, making it inaccessible even through official channels. Finally, for some periods, locations, and variables, the data simply has not been collected.

For headwater watersheds serving as a supply for heavy demand downstream, similar to the Sasumua River Watershed, knowledge of projected changes in streamflow is crucial for the design of dam and diversion infrastructure and for planning mitigation strategies for areas of increased flood risk. Without daily data on flows through streams and diversions, the precision of hydrologic estimates will be low, which leads to unanticipated risks that could have been averted and superfluous investments in protective measures should risks be overestimated. To accommodate interest in surface water and groundwater quality studies, it will be essential to increase the capacity of current water quality monitoring networks. Periodic data on water table levels and chemical concentrations could vastly improve approximations of groundwater quality status for more effective planning and modelling efforts.

Volume 1 of the World Meteorological Organization (WMO) Guide to Hydrological Practice has suggested that the value of data stems directly from its use, implying that a financial loss is incurred when data is collected and cannot be used to its full potential (WMO, 2020). The guide also emphasizes the importance of coordinated data collection efforts and planning towards integrated data networks. Explicit data policies will need to be established to improve intra- and international communication and sharing between agencies collecting data that could inform water resources management nationally and globally.

Discussion with practitioners in the watershed indicated a strong push towards transitioning to automated data collection methods for gauge data, which will increase the capacity for real-time data capture and reporting. With these new initiatives come new

opportunities for data policies that support hydrological and climate research. This includes making centralized databases with public catalogs of datasets in their inventory. Additionally, improvements could be made in the documentation of instruments and procedures used to collect data—information highly relevant to analysis and modelling when quantifying uncertainty of inputs and results (Saraswat et al., 2015). These actions correspond well with the theme "Strengthening of Hydrometeorological Information Management", which is part of the strategy for capacity development outlined in Kenya's National Water Master Plan 2030 (Nippon Koei Co., Ltd, 2013). Current systems for gaining access to meteorological and hydrological data in Kenya rely on data request forms that have varying response rates and are challenging to use without preexisting knowledge of what datasets are available. Ideally, datasets would be organized in a portal where they would be downloadable by any interested individual. However, if data access is restricted, researchers at national and international education institutions and non-profit organizations should have a simple, efficient, and clearly defined pathway to gaining access.

## 4 Conclusions

While model outputs are useful for decision-making when presented in relative terms, current data collection and dissemination systems for this watershed and the greater region of East Africa do not address the critical need for data. In the coming decades, the Sasumua River watershed is projected to experience increased rainfall and streamflow under the climate scenarios SSP2/RCP4.5, SSP3/RCP7.0, and SSP4/RCP8.5. Based on mean annual results, by the year 2090 and under the same diversion scheme, this flow difference may be as much as three times the current amount, with moderate climate scenarios producing an increase of over double the baseline amount. Thus, making and managing water resources decisions will become even more critical into the future. Current indications suggest that the most effective management scenario for reduction in mean annual sediment, organic nitrogen, and organic phosphorous yields and $NO_3$ in runoff is that which combines a variety of practices, with the most effective single management practice being the application of filter strips. The unavailability of daily measured data for the study watershed, however, presents a challenge, for example, by

introducing uncertainties into the modeling and decision-making process. Likewise, the lack of readily usable groundwater data makes any results pertaining to groundwater an estimate, at best. Unfortunately, this situation is not unique to the study watershed, rather, is common within the greater East Africa region. Meeting the need for available and accessible water and climate data will reduce the uncertainty of results and increase the representativeness of specific results such as flow rates and pollutant concentrations for use in water resources decision-making and management and, ultimately, in improving water security in the region.

**Funding:** This work was funded in part by the LASER-PULSE program through USAID's Innovation, Technology, and Research Hub.

## 5 References

Affessa, G.M., Belew, A.Z., Tenagashaw, D.Y., Tamirat, D.M., 2022. Land Use/Cover Change Impacts on Hydrology Using SWAT Model on Borkena Watershed, Ethiopia. Water Conserv. Sci. Eng. 7(1), 55–63. https://doi.org/10.1007/s41101-022-00128-1

Alemayehu, T., van Griensven, A., Bauwens, W., 2016. Evaluating CFSR and WATCH Data as Input to SWAT for the Estimation of the Potential Evapotranspiration in a Data-Scarce Eastern-African Catchment. J. Hydrol. Eng. 21(3), 5015028–. https://doi.org/10.1061/(ASCE)HE.1943-5584.0001305

Alipour, M.H., Kibler, K.M., 2019. Streamflow prediction under extreme data scarcity: a step toward hydrologic process understanding within severely data-limited regions. Hydrol. Sci. J. 64(9), 1038–1055. https://doi.org/10.1080/02626667.2019.1626991

Archer, D., 1996. Suspended sediment yields in the Nairobi area of Kenya and environmental controls, in: Walling, D.E. & Webb, B.W. (Eds.), Erosion and sediment yield: global and regional perspectives. Proc. Exeter Symp. July 1996, Vol. 236, 37–48.

Arnold, J.G., Srinivasan, R., Muttiah, R.S., Williams, J.R., 1998. Large area hydrologic modeling and assessment part I: Model development. J. Am. Water Resour. Assoc. 34(1), 73–89. https://doi.org/10.1111/j.1752-1688.1998.tb05961.x

Bailey, R.T., Park, S., Bieger, K., Arnold, J.G., Allen, P.M., 2020. Enhancing SWAT+ simulation of groundwater flow and groundwater-surface water interactions using MODFLOW routines. Environ. Modell. Software 126, 104660. https://doi.org/10.1016/j.envsoft.2020.104660

Batjes, N.H., Gicheru, P., 2004. Soil data derived from SOTER for studies of carbon stocks and change in Kenya (GEF-SOC Project; Version 1.0), Technical Report 2004/01. ISRIC – World Soil Information, Wageningen.

https://www.isric.org/sites/default/files/isric_report_2004_01.pdf (accessed 26 April 2022).

Bieger, K., Arnold, J.G., Rathjens, H., White, M.J., Bosch, D.D., Allen, P.M., Volk, M., Srinivasan, R., 2017. Introduction to SWAT+, A Completely Restructured Version of the Soil and Water Assessment Tool. J. Am. Water Resour. Assoc. 53(1), 115–130. https://doi.org/10.1111/1752-1688.12482

[dataset] Buchhorn, M., Smets, B., Bertels, L., Lesiv, M., Tsendbazar, N.-E., Masiliunas, D., Linlin, L., Herold, M., Fritz, S., 2020. Copernicus Global Land Service: Land Cover 100m: Collection 3: epoch 2015: Globe (Version V3.0.1). Zenodo. https://doi.org/10.5281/zenodo.3939038

Cook, K.H., Fitzpatrick, R.G.J., Liu, W., Vizy, E.K., 2020. Seasonal asymmetry of equatorial East African rainfall projections: understanding differences between the response of the long rains and the short rains to increased greenhouse gases. Clim. Dyn. 55, 1759–1777. https://doi.org/10.1007/s00382-020-05350-y

County Government of Nyandarua, 2018. Nyandarua County Integrated Development Plan (CIDP2) 2018-2022. https://repository.kippra.or.ke/handle/123456789/663 (accessed 15 March 2022).

Chaubey, I., Chiang, L., Gitau, M.W., Mohamed, S., 2010. Effectiveness of best management practices in improving water quality in a pasture-dominated watershed. J. Soil Water Conserv. 65(6), 424–437. https://doi.org/10.2489/jswc.65.6.424

Dijkshoorn J.A., Macharia P.N., Huting J.R.M., Maingi P.M., Njoroge C.R.K., 2011. Soil and terrain conditions for the Upper Tana River catchment, Kenya. (ver1.1). Green Water Credits Report 11 / ISRIC Report 2010/09b, ISRIC – World Soil Information, Wageningen. https://isric.org/sites/default/files/isric_report_2010_09b.pdf

Dinku, T., Asefa, K., Hilemariam, K., Grimes, D., Connor, S., 2011. Improving availability, access and use of climate information. WMO Bull. 60(2), 80–86. https://library.wmo.int/doc_num.php?explnum_id=7013. (accessed 25 April 2022).

Dixon, H. H. & Berry, D.W (1970) Extensions to the Chania-Sasuma water supply scheme for Nairobi. Proc. Inst. Civ. Eng. 45(1), 35–64. https://doi.org/10.1680/iicep.1970.7204

Garibay, V.M., Gitau, M.W., Kongo, V., Kisekka, J., Moriasi, D., 2022. Comparative Evaluation of Water Resource Data Policy Inventories Towards the Improvement of East African Climate and Water Data Infrastructure. Water Resour. Manage. 36(11), 4019–4038. https://doi.org/10.1007/s11269-022-03231-z

Ghimire, S.R., Johnston, J.M., 2013. Impacts of domestic and agricultural rainwater harvesting systems on watershed hydrology: A case study in the Albemarle-Pamlico river basins (USA). Ecohydrol. Hydrobiol. 13(2), 159–171. https://doi.org/10.1016/j.ecohyd.2013.03.007

Gitau, M.W., Chaubey, I., 2010. Regionalization of SWAT Model Parameters for Use in Ungauged Watersheds. Water (Basel) 2(4), 849–871. https://doi.org/10.3390/w2040849

Gitau, M.W., Veith, T.L., Gburek, W. J., Jarrett, A.R., 2006. Watershed level best management practice selection and placement in the town brook watershed, New York. J. Am. Water Resour. Assoc. 42(6), 1565–1581.

Hall, J.W., Meadowcroft, I.C., Sayers, P.B., Bramley, M.E., 2003. Integrated Flood Risk Management in England and Wales. Nat. Hazard. Rev. 4(3), 126–135. https://doi.org/10.1061/(ASCE)1527-6988(2003)4:3(126)

Hengl, T., Mendes de Jesus, J., Heuvelink, G.B.M., Ruiperez Gonzalez, M., Kilibarda, M., Blagotić, A., Shangguan, W., Wright, M.N., Geng, X., Bauer-Marschallinger, B., Guevara, M.A., 2017. SoilGrids250m: Global gridded soil information based on machine learning. PLoS ONE, 12(2), e0169748. https://doi.org/10.1371/journal.pone.0169748

Hunink, J.E., Droogers, P., 2011. Physiographical baseline survey for the Upper Tana catchment: erosion and sediment yield assessment. Future Water Rep. 112, 31. https://futurewater.nl/wp-content/uploads/2013/01/2011_TanaSed_FW-1121.pdf (accessed 7 January 2022)

Jaetzold, R., Schmidt, H., Hornetz, B., Shisanya, C., 2006. Farm management handbook of Kenya: Volume II: Natural conditions and farm management information; Part B: Central Kenya; Subpart B2: Central Province (2nd ed.). Kenya Ministry of Agriculture. https://star-www.giz.de/fetch/88Xl00jdWg0001Q1JV/07-1284.pdf (accessed 24 March 2022)

Khaing, Z.M., Zhang, K., Sawano, H., Shrestha, B.B., Sayama, T., Nakamura, K., 2019. Flood hazard mapping and assessment in data-scarce Nyaungdon area, Myanmar. PLoS One 14(11): e0224558. https://doi.org/10.1371/journal. pone.022455

Kwakye, S.O., Bárdossy, A., 2020. Hydrological modelling in data-scarce catchments: Black Volta basin in West Africa. Springer Nat. Appl. Sci. 2, 628. https://doi.org/10.1007/s42452-020-2454-4

Kyei, E., 2020. Land use change and soil erosion assessment: the case of Sasumua catchment in Kenya. ResearchGate. https://doi.org/10.13140/RG.2.2.22674.68803/3

Liu, W., Park, S., Bailey, R.T., Molina-Navarro, E., Andersen, H.E., Thodsen, H., Nielsen, A., Jeppesen, E., Jensen, J.S., Jensen, J.B., Trolle, D., 2020. Quantifying the streamflow response to groundwater abstractions for irrigation or drinking water at catchment scale using SWAT and SWAT–MODFLOW. Environ. Sci. Eur. 32(1). https://doi.org/10.1186/s12302-020-00395-6

Mirdashtvan, M., Najafinejad, A., Malekian, A., Sa'doddin, A., 2021. Sustainable Water Supply and Demand Management in Semi-arid Regions: Optimizing Water Resources Allocation Based on RCPs Scenarios. Water Resour. Manage. 35(15), 5307–5324. https://doi.org/10.1007/s11269-021-03004-0

Mwangi, J.K., Shisanya, C.A., Gathenya, J.M., Namirembe, S., Moriasi, D.N., 2015. A modeling approach to evaluate the impact of conservation practices on water and sediment yield in Sasumua watershed, Kenya. J. Soil Water Conserv. 70(2), 75–90. https://doi.org/10.2489/jswc.70.2.75

Nakaegawa, T., Wachana, C., KAKUSHIN Team-3 Modeling Group, 2012. First impact assessment of hydrological cycle in the Tana River Basin, Kenya, under a changing climate in the late 21st Century. Hydrol. Res. Lett. 6, 29–34. https://doi.org/10.3178/hrl.6.29

[dataset] NASA JPL, 2013. NASA Shuttle Radar Topography Mission Global 1 arc second. NASA EOSDIS Land Processes DAAC. https://doi.org/10.5067/MEaSUREs/SRTM/SRTMGL1.003

Nduhiu, C., Gathenya, J.M., Mwangi, J.K., Aman, M., Mutisya, T., 2016. Assessment of the effectiveness of Payment for Ecosystem Services (PES) in the delivery of desired Ecosystem Services in Sasumua catchment, Kenya. Hydrol. Earth Syst. Sci. Discuss. 1–20. https://doi.org/10.5194/hess-2016-541

Nippon Koei Co., Ltd (for Japan International Cooperation Agency), 2013. Proposed Action Plans Toward 2022. In National Water Master Plan 2030, Vol. III, Part H. https://wasreb.go.ke/national-water-master-plan-2030/ (accessed 24 April 2022).

Noteboom, M., Seidou, O., Lapen, D.R., 2021. Predicting water quality trends resulting from forest cover change in an agriculturally dominated river basin in Eastern Ontario, Canada. Water Qual. Res. J. 56(4), 218–238. https://doi.org/10.2166/wqrj.2021.010

O'Neill, B.C., Tebaldi, C., van Vuuren, D.P., Eyring, V., Friedlingstein, P., Hurtt, G., Knutti, R., Kriegler, E., Lamarque, J.-F., Lowe, J., Meehl, G.A., Moss, R., Riahi, K., Sanderson, B.M., 2016. The Scenario Model Intercomparison Project (ScenarioMIP) for CMIP6, Geosci. Model Dev. 9, 3461–3482, https://doi.org/10.5194/gmd-9-3461-2016.

Oseko, E., Dienya, T., 2015. Fertilizer consumption and fertilizer use by crop (FUBC) in Kenya. https://africafertilizer.org/wp-content/uploads/2017/05/FUBC-Kenya-final-report-2015.pdf (accessed 26 April 2022)

Penatti, N.C., de Almeida, T.I.R., Ferreira, L.G., Arantes, A.E., Coe, M.T., 2015. Satellite-based hydrological dynamics of the world's largest continuous wetland. Remote Sens. Environ. 170, 1–13. https://doi.org/10.1016/j.rse.2015.08.031

Riahi, K., van Vuuren, D.P., Kriegler, E., Edmonds, J., O'Neill, B.C., Fujimori, S., Bauer, N., Calvin, K., Dellink, R., Fricko, O., Lutz, W., Popp, A., Cuaresma, J.C., KC, S., Leimbach, M., Jiang, L., Kram, T., Rao, S., Emmerling, J., Ebi, K., Hasegawa, T., Havlik, P., Humpenoder, F., Da Silva, L.A., Smith, S., Stehfest, E., Bosetti, V., Eom, J., Gernaat, D., Masui, T., Rogelj, J., Strefler, J., Drouet, L., Krey, V., Luderer, G., Harmsen, M., Takahashi, K., Baumstark, L., Doelman, J.C., Kainuma, M., Klimont, Z., Marangoni, G., Lotze-Campen, H., Obersteiner, M., Tabeau, A., Tavoni, M., 2016. The Shared Socioeconomic Pathways and their energy, land use, and greenhouse gas

emissions implications: An overview. Global Environ. Change 42, 153–168. https://doi.org/10.1016/j.gloenvcha.2016.05.009

Rocha, J., Duarte, A., Silva, M., Fabres, S., Vasques, J., Revilla-Romero, B., Quintela, A., 2020. The Importance of High Resolution Digital Elevation Models for Improved Hydrological Simulations of a Mediterranean Forested Catchment. Remote Sens. (Basel) 12(20), 3287–. https://doi.org/10.3390/rs1220

[dataset] Saha, S., Moorthi, S., Pan, H., Wu, X., Wang, J., Nadiga, S., Tripp, P., Kistler, R., Woollen, J., Behringer, D., Liu, H., Stokes, D., Grumbine, R., Gayno, G., Wang, J., Hou, Y., Chuang, H., Juang, H.H., Sela, J., Iredell, M., Treadon, R., Kleist, D., Van Delst, P., Keyser, D., Derber, J., Ek, M., Meng, J., Wei, H., Yang, R., Lord, S., van den Dool, H., Kumar, A., Wang, W., Long, C., Chelliah, M., Xue, Y., Huang, B., Schemm, J., Ebisuzaki, W., Lin, R., Xie, P., Chen, M., Zhou, S., Higgins, W., Zou, C., Liu, Q., Chen, Y., Han, Y., Cucurull, L., Reynolds, R.W., Rutledge, G., Goldberg, M., 2010. NCEP Climate Forecast System Reanalysis (CFSR) 6-hourly Products, January 1979 to December 2010. Research Data Archive at the National Center for Atmospheric Research, Computational and Information Systems Laboratory. https://doi.org/10.5065/D69K487J.

[dataset] Saha, S., Moorthi, S., Wu, X., Wang, J., Nadiga, S., Tripp, P., Behringer, D., Hou, Y., Chuang, H., Iredell, M., Ek, M., Meng, J., Yang, R., Mendez, M.P., van den Dool, H., Zhang, Q., Wang, W., Chen, M., Becker, E., 2011 (updated daily). NCEP Climate Forecast System Version 2 (CFSv2) 6-hourly Products. Research Data Archive at the National Center for Atmospheric Research, Computational and Information Systems Laboratory. https://doi.org/10.5065/D61C1TXF.

Saraswat, D., Frankenberg, J.R., Pai, N., Ale, S., Daggupati, P., Douglas-Mankin, K.R., Youssef, M.A., 2015. Hydrologic and water quality models: Documentation and reporting procedures for calibration, validation, and use. Trans. ASABE 58(6), 1787-1797. http://dx.doi.org/10.13031/trans.58.10707

Seibert, J., McDonnell, J.J., 2002. On the dialog between experimentalist and modeler in catchment hydrology: Use of soft data for multicriteria model calibration. Water Resour. Res. 38(11), 23–1–23–14. https://doi.org/10.1029/2001WR000978

Sinclair, A., Jamieson, R., Madani, A., Gordon, R. J., Hart, W., Hebb, D., 2014. A Watershed Modeling Framework for Phosphorus Loading from Residential and Agricultural Sources. J. Environ. Qual. 43(4), 1356–1369. https://doi.org/10.2134/jeq2013.09.0368

Sholichin, M., Qadri, W., 2020. Predicting flood hazards area using swat and hec-ras simulation in Bila river, South Sulawesi. IOP Conf. Ser.: Earth Environ. Sci. 437(1), 12055–. https://doi.org/10.1088/1755-1315/437/1/012055

Smit, E., van Tol, J., 2022. Impacts of Soil Information on Process-Based Hydrological Modelling in the Upper Goukou Catchment, South Africa. Water (Basel), 14(3), 407–. https://doi.org/10.3390/w14030407

Wilkinson, M.D., Dumontier, M., Aalbersberg, I.J., Appleton, G., Axton, M., Baak, A., Blomberg, N., Boiten, J.W., da Silva Santos, L.B., Bourne, P.E., Bouwman, J., 2016. The FAIR Guiding Principles for scientific data management and stewardship. Sci. Data 3(1), 1-9. https://doi.org/10.1038/sdata.2016.18

WMO, 2020. Guide to Hydrological Practices Volume I: Hydrology—From Measurement to Hydrological Information (2008 ed.) World Meteorological Organziation. WMO-No. 168. https://library.wmo.int/doc_num.php?explnum_id=10473 (accessed 10 March 2022).

Yang, Q., Zhao, Z., Chow, T.L., Rees, H.W., Bourque, C. P.-A., Meng, F.-R., 2009. Using GIS and a digital elevation model to assess the effectiveness of variable grade flow diversion terraces in reducing soil erosion in northwestern New Brunswick, Canada. Hydrol. Processes 23(23), 3271–3280. https://doi.org/10.1002/hyp.7436

END OF MANUSCRIPT

SUPPLEMENTARY MATERIAL

# APPENDIX I: CASE STUDY METHODS SUPPLEMENT

## Data Development

### *Topography*

The digital elevation model (DEM) was sourced from the Shuttle Radar Topography Mission (SRTM) global 1 arc-second version 003 product provided through collaborative efforts organized by NASA (NASA JPL, 2013). The raster images are available as zipped granule files in the NASA EarthData portal (Earthdata Search). After creation of a free account, granules can be downloaded individually and are named according to the coordinate at the bottom left corner of the 1° x 1° bounding box represented in the tile (e.g., S01E036.SRTMGL1.hgt.zip for this case study). The portal also offers spatial filtering tools for the identification of relevant granules. The DEM resolution is approximately 30 m.

### *Land Cover*

The discrete classification Copernicus Global Land Cover 100m products (Buchhorn et al., 2020) for the years 2015 and 2019 were downloaded using the Global Land Cover Viewer (Land Cover Viewer), where they are available in 20° x 20° tiles. To develop these land cover maps an algorithm summarizes satellite imagery into 23 discrete classes on an annual basis. After downloading the discrete classification land cover file for 2015 and 2019 for tile E20 N20, the 2015 map was used in QGIS to prepare the model, the basin outline from the QSWAT+ setup was saved as a shapefile. This shapefile was used to clip the 2015 and 2019 land use rasters (with preserve input layer resolution checked) in a separate QGIS3 document. These clipped rasters were processed with the raster layer histogram tool to determine the pixel count for each land cover class. The comparison of the counts as well as the percentage of the total map they comprise for each of the years is shown in the table below (Table S1). Examination of the changes in land cover over the 5-year period revealed that changes for all categories were equivalent 0.1% of the total area or less. The original 2015 tile was clipped to the extent of the DEM for use in the model. The land cover map resolution is approximately 100 m.

**Table S1.** Pixel count and percent of total area for Copernicus Global Land Cover 100m from 2015 to 2019 and change in percent of total area from 2015 to 2019.

| SWAT Landuse | 2015 | | 2019 | | Δ Percent |
|---|---|---|---|---|---|
| | Pixel count | Percent (%) | Pixel count | Percent (%) | |
| RNGB | 40 | 0.4 | 39 | 0.3 | 0.0 |
| WETL | 226 | 2.0 | 211 | 1.9 | -0.1 |
| AGRL | 4586 | 40.6 | 4583 | 40.6 | 0.0 |
| URML | 85 | 0.8 | 85 | 0.8 | 0.0 |
| WATR | 23 | 0.2 | 32 | 0.3 | 0.1 |
| WETN | 51 | 0.5 | 56 | 0.5 | 0.0 |
| FRSE | 4117 | 36.4 | 4123 | 36.5 | 0.1 |
| FRST | 1025 | 9.1 | 1025 | 9.1 | 0.0 |
| FRSE | 265 | 2.3 | 268 | 2.4 | 0.0 |
| FRST | 880 | 7.8 | 876 | 7.8 | 0.0 |

*Soils*

The International Soil Reference and Information Centre (ISRIC) has developed a series of Soil and Terrain (SOTER) databases at various levels. The primary map and database used for the model was the Upper Tana SOTER (SOTER_UT, Dijkshoorn et al., 2011) product, a derivative of an earlier Kenya SOTER (KENSOTER) product, which incorporated more regional studies and surveys of the Upper Tana region. Since the watershed delineation did not perfectly coincide with the delineation used in developing SOTER_UT, a few missing segments were sourced from the most recent version of KENSOTER (version 2.0, Batjes & Gicheru, 2004). Not all of the soil profiles relevant to the model had every variable documented as required by SWAT+, requiring additional development (Tables S2 & S3). Whenever possible, the available information was used with reference tables or pedotransfer functions to estimate any missing variables. For variables such as organic carbon, to which these techniques did not apply, the corresponding ISRIC SoilGrids250m GeoTIFFs (Hengl et al., 2017) for each depth level within the range of the soil profile were clipped to match the spatial extent of the profile, and the average pixel value within that polygon was applied to the soil profile for that depth. Layers were added in cases where the depths did not correspond with existing layers in the profile. SOTER_UT, has an approximate resolution of 125m, but data was also incorporated from maps with an effective resolution as coarse as 500 m.

**Table S2.** Soil profile development details.

| Variable | Procedure for Missing Values |
|---|---|
| Organic Carbon (OC) | In QGIS 3.18.1 Zonal Statistics were calculated for the soil organic carbon layers from ISRIC SoilGrids250m on the basis of the soil group polygons from the merged SOTER shapefile. For soil groups with multiple polygons, area weighted averages of the mean for each polygon were used in the soil profile. Where layer depths in the soil profile did not align with the SoilGrids 250 layers, the existing soil profile layers were subdivided to accommodate the two different values. Units for SoilGrids are (dg/kg). Units for SOTER are g/kg. The necessary conversions were made to achieve the percent soil weight (g/kg) required by SWAT. |
| Bulk Density (BD) | Populated using the equation from Hong et al. (2013): $BD = 1.02 - 0.156 * \log_{10}(OM)$, where $OM$ is organic matter content in g/100g. |
| Electrical Conductivity (EC) | Populated with the default value of 0. Arnold et al. (2013) suggests that EC is not in use. |
| Available Water Capacity (AWC) | Populated using the equation: $AWC = SM_{-33\,kPa} - SM_{-1500\,kPa}$ where $SM$ is soil moisture at the tensions designated in the subscript (adapted from O'Geen, 2013). In cases where these values for the layer were unavailable, the following equations adapted from Saxton & Rawls (2006) were used: $SM_{-1500\,kPa} = (-0.024 * Sand + 0.487 * Clay + 0.006 * OC * 1.72 + 0.005 * Sand * OC * 1.72 + 0.068 * Sand * Clay + 0.031) + (0.14 * -.024 * Sand + 0.487 * Clay + 0.006 * OC * 1.72 + 0.005 * Sand * OC * 1.72 - 0.013 * Clay * OC * 1.72 + 0.068 * Sand * Clay + 0.031) - 0.02$, where $Sand$, $Clay$, and $OC$ are the percentages of sand, clay, and organic carbon in the soil, respectively. An assumption was made that organic matter from these equations did not refer to only the organic carbon component of organic matter so a 1.72 conversion factor was applied (Arnold et al., 2013). |
| Albedo | Populated using the equation from Post et al. (2000): $Albedo = 0.069 * ColorValue - 0.114 * 0.93$, where ColorValue is the number before the slash in Munsell notation. |

## **Table S2.** continued

| | |
|---|---|
| $K_{sat}$ | Populated using the equations:<br>$K_{sat} = 10 * \exp\left[12.012 - 0.0755 * Sand + \left(-3.8950 + 0.03671 * Sand - 0.1103 * Clay + 8.7546 * 10^{-4} * Clay^2\right) * \left(0.332 - 7.251 * 10^{-4} * Sand + 0.1276 * \log_{10}(Clay)\right)^{-1}\right]$,<br>where *Sand* and *Clay* are the percentages of sand and clay in the soil (Saxton et al., 1986). |
| $K_{USLE}$ | Populated using the equation:<br>$K_{USLE} = \left(0.2 + 0.3 * \exp\left(-0.256 * Sand * \left(1 - \frac{Silt}{100}\right)\right)\right) * \left(\frac{Silt}{Clay + Silt}\right)^{0.3} * \left(1 - \left(\frac{0.0256 * OC * 1.72}{OC + \exp(3.72) - 2.95 * OC}\right)\right) * \left(1 - \frac{0.7 * \left(1 - \left(\frac{Sand}{100}\right)\right)}{1 - \frac{Sand}{100} + \exp\left(-5.51 + 22.9 * \left(1 - \frac{Sand}{100}\right)\right)}\right)$,<br>based on the method from Williams (1995) as cited in Arnold et al. (2013) where *Sand*, *Silt*, *Clay*, and *OC* are the percentages of sand, silt, clay, and organic carbon in the soil. |
| Rock | For profiles with letter classifications, the average of the percentage range was acquired from Table S3. For remaining profiles, the zonal statistics procedure used to estimate *OC* was applied to the relevant SoilGrids250m Coarse Fragments Volumetric layers. Since both SOTER classifications and SoilGrids resulted in a volumetric fraction in $cm^3/dm^3$, it was necessary to convert this to a weight fraction (for use with SWAT) using the bulk soil density for each profile and layer. For this conversion, a fragment density of $2.7 g/cm^3$ was used. |
| Hydrologic Soil Group (HSG) | HSG assignment was based on $K_{sat}$ values under the guidelines in Mockus et al. (2009). |

**Table S3.** Volume Percentages of Rock and Coarse Fragments (adapted from Van Engelen & Dijkshoorn, 2012).

| Class | Description | Percentage Range | Average |
|---|---|---|---|
| N | None | 0% | 0% |
| V | Very Few | 0-2% | 1% |
| F | Few | 2-5% | 3.5% |
| C | Common | 5-15% | 10% |
| M | Many | 15-40% | 27.5% |
| A | Abundant | 40-80% | 60% |
| D | Dominant | >80% | 90% |

*Climate*

Past studies indicate that the study site has three active weather stations: 9036152 South Kinangop Njabini Farmers Training Centre (-0.72, 36.65), 9036164 South Kinangop Forest (-0.72, 36.68), and 9036188 Sasumua Dam (-0.75, 36.67). However, it was not possible to procure observed meteorological data on a daily time scale for this study; multiple requests for daily data from specific stations within and near the watershed were not successful despite the efforts of those committed to assisting with this research. To proceed with the case study, daily precipitation and temperature range data for the period 1979-2021 was retrieved for the most proximate grid point (-0.50, 36.50) to Station 9036152 from the CFSR database (Saha et al., 2010; Saha et al., 2011) for use with model calibration and validation. While not equivalent to measured data, the CFSR is commonly used in research as a source of reliable daily meteorological data (Garibay et al., 2021). Monthly precipitation data for Station 9036152 sourced from the Kenya Water Resources Authority (WRA) was used to confirm the suitability of the CFSR data for the study based on mean and distribution comparison for monthly totals for the years with data available (1979-1993 excluding two months without observations, Fig. S1a). The monthly precipitation totals matched well for the first dry season, were a mixed under- and over- prediction for the long rains, overpredicted the second dry season through October, and were representative of the means for the remainder of the short rains season. Overall, representation of seasonal trends was preserved, and the CFSR datasets were used with the expectation of slightly inflated annual precipitation, most notably increased for the second dry season. A comparison of minimum and maximum temperature summaries from the KENSOTERv2 database for Station 9036152 sourced from the Kenya Meteorological department for the year range 1959-1964 to CFSR

temperature data for the modelling period, 2011-2020, revealed an overall increase in minimum temperatures and an increase in maximum temperatures, particularly for February-April, September, and October. This is consistent with expectations for changes in climate over the approximate five-decade gap between the two periods (Fig. S1b).

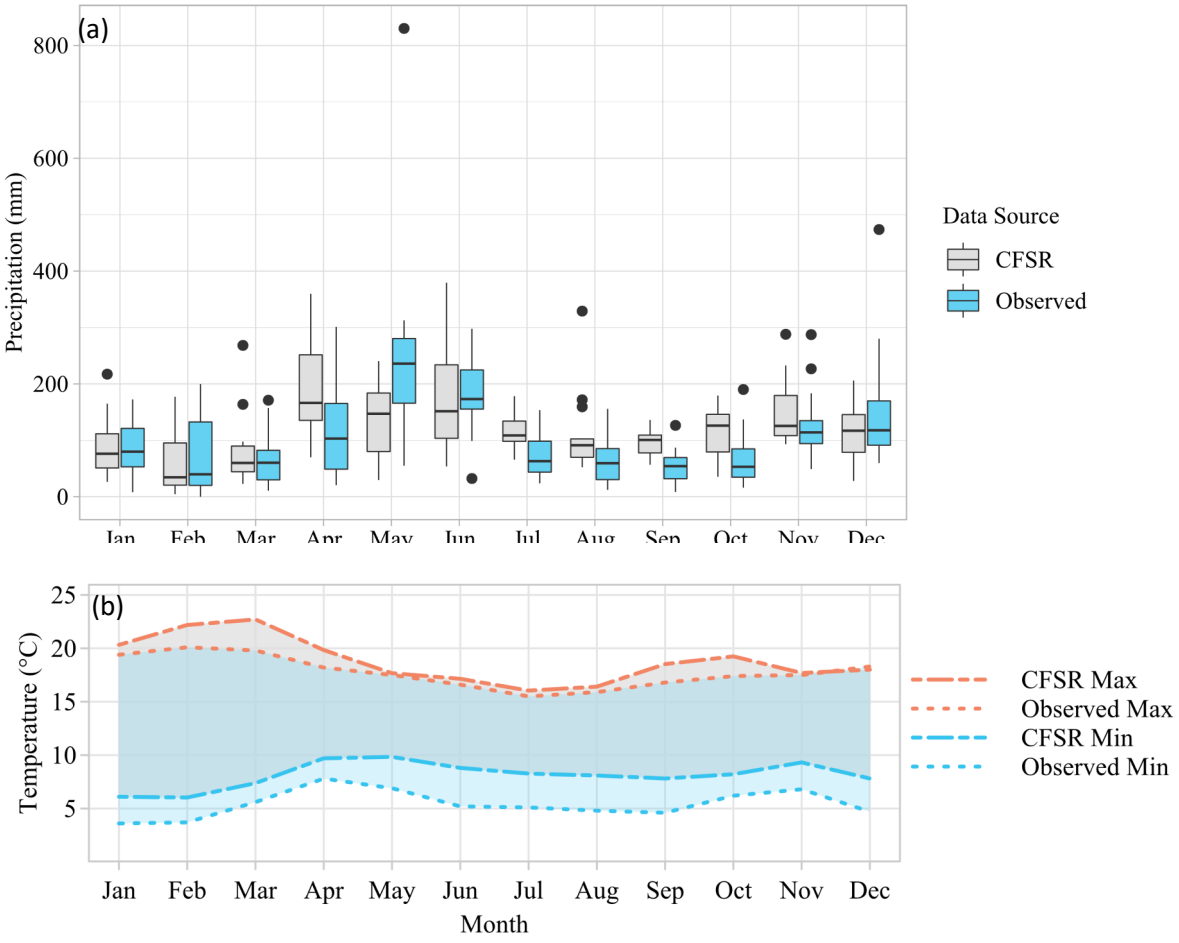


**Figure S1** (a) Comparison of total monthly precipitation for the years 1979-1993 for observed data from Njabini (Station 9036152) and CFSR data (Grid Point 0.5S 36.5E). Points represent statistical outliers and are not considered in the formation of the boxplots. (b) Comparison of mean monthly observed minimum and maximum temperatures for the period 1959-1964 from Njabini (Station 9036152) and mean monthly CFSR minimum and maximum temperatures for the period 2011-2020.

*Future Time Series*

Projected climate data for precipitation and temperature range was retrieved for a selection of seven model outputs from the Coupled Model Intercomparison Project Phase 6 (CMIP6, O'Neill et al., 2016). Scenarios for CMIP6 are representative of different Shared Socioeconomic Pathways (SSPs), which embody variations in global adaptation responses to climate change, and Representative Concentration

Pathways (RCPs), which reflect differences in greenhouse gas concentration trajectories. The seven models used in this study are the continuous subset of models available at daily, 100-m resolution for precipitation and surface temperature extremes for all four of the considered climate scenarios (Garibay et al, 2022). The general societal behaviors characterized by the SSPs featured are 1, sustainability-conscious development; 2, moderate/mixed development approach; 3, low prioritization of environmental concerns; and 5 growth driven by fossil-fuels (Riahi et al., 2016). A summary of the characteristics for each model across SSPs is provided in Table S4. An overview of differences in CMIP6 model outputs for SSP2/RCP4.5 between the past decade and the remaining 80 years suggests that maximum monthly precipitation may increase, with the greatest changes occurring in April and throughout the short rains season (Fig. S2); minimum temperature ranges are likely to remain fairly consistent over time (Fig. S3), while the upper limit of projected maximum temperature ranges is likely to increase (Fig. S4).

The CMIP6 model outputs were used as climate inputs in the calibrated SWAT+ project to predict the effects of climate change on discharge into the Sasumua Reservoir considering the periods: 2011-2020 (baseline) and successive twenty-year periods in the near, middle, and distant future (2031-2050, 2051-2070, and 2071-2090, respectively). The calibrated SWAT+ model—anchored on the baseline scenario—was run with data from each of the CMIP6 models for SSP1/RCP2.6, SSP2/RCP4.5, SSP3/RCP7.0, and SSP5/RCP8.5, for a total of 28 SWAT model outputs.

**Table S4** Range of change in mean annual values for the period 2071-2100 against a baseline 1991-2020 climate normal for seven CMIP6 model outputs under SSPs 1, 2, 3, and 5 for the most proximate grid point to Njabini (Station 9036152) in the Sasumua River Watershed.

| Model | Δ Total Precipitation (%) | Δ Number of days receiving rainfall in excess of the baseline 95$^{th}$ percentile (%) | Δ Minimum Surface Air Temperature (°C) | Δ Maximum Surface Air Temperature (°C) |
|---|---|---|---|---|
| CMCC-ESM2 | (35.7%, 50.3%) | (48.6%, 60.3%) | (1.1°C, 2.1°C) | (0.9°C, 3.1°C) |
| GFDL-ESM4 | (-11.1%, 6.7%) | (-20.9%, 10.3%) | (0.9°C, 2.7°C) | (0.9°C, 3.5°C) |
| INM-CM4.8 | (2.2%, 15.8%) | (-2.8%, 29.6%) | (0.6°C, 2.8°C) | (0.8°C, 3.1°C) |
| INM-CM5.0 | (2.4%, 15%) | (5.5%, 45.4%) | (0.7°C, 2.5°C) | (0.9°C, 2.3°C) |
| MPI-ESM1.2-HR | (-6%, 4.9%) | (-8.2%, 13%) | (0.7°C, 3.8°C) | (0.8°C, 2.6°C) |
| NorESM2-MM | (7.3%, 23.1%) | (8.1%, 25.5%) | (1°C, 3.4°C) | (1.1°C, 3.2°C) |
| TaiESM1 | (28.1%, 44.4%) | (29.8%, 53.3%) | (-1.4°C, 0.3°C) | (5.4°C, 8.2°C) |

*Footnote:* Shared Socioeconomic Pathways (SSPs) 1-Sustainability; 2-Middle of the Road; 3-Regional Rivalry; 5-Fossil-Fueled Development

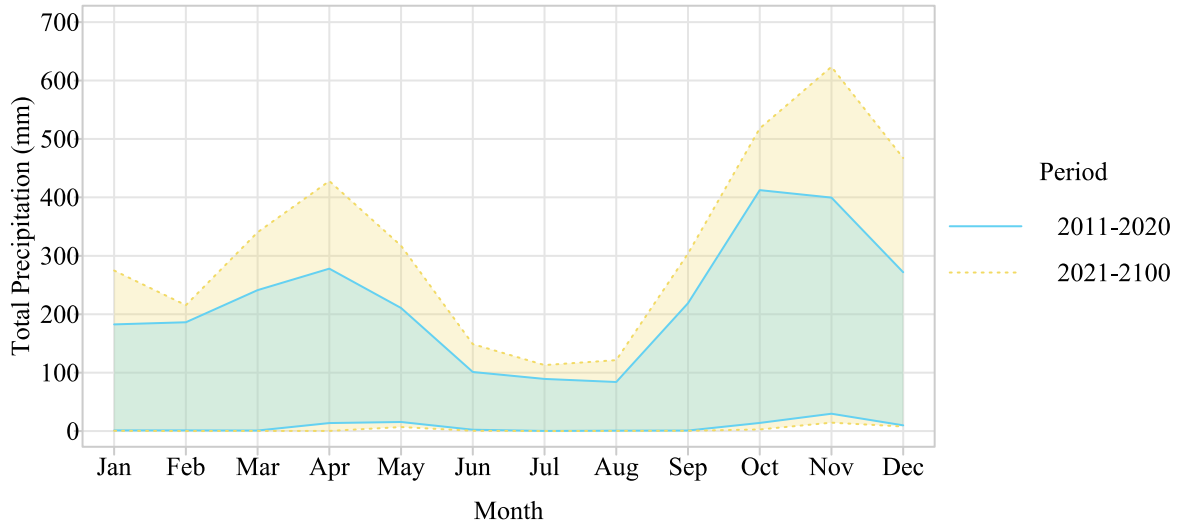


**Figure S2** Comparison of span of monthly precipitation outputs for seven CMIP6 models under SSP2/RCP4.5 during the periods 2011-2020 and 2021-2100.

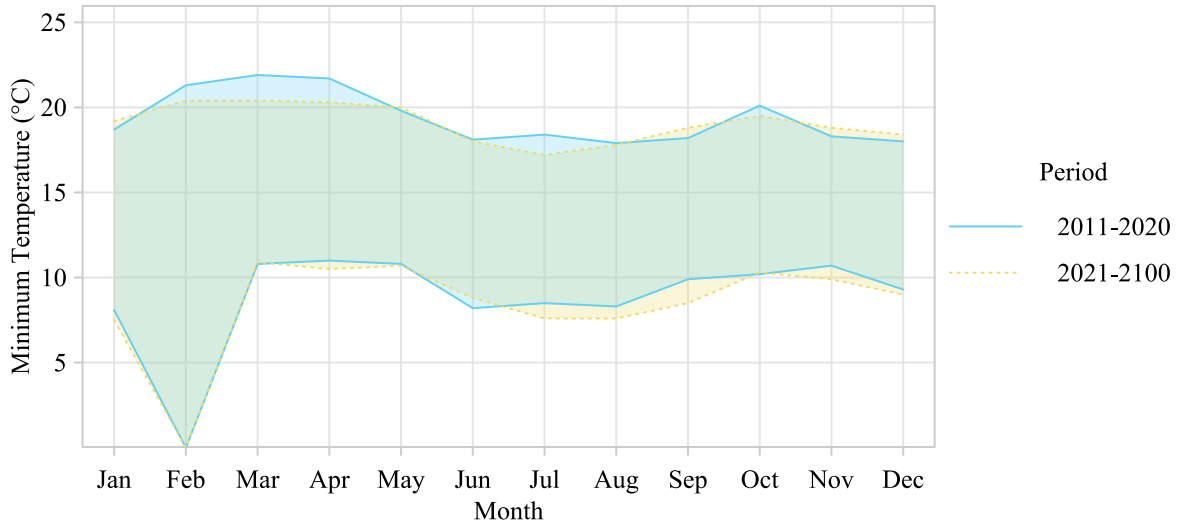


**Figure S3** Comparison of span of monthly minimum temperature outputs for seven CMIP6 models under SSP2/RCP4.5 during the periods 2011-2020 and 2021-2100.

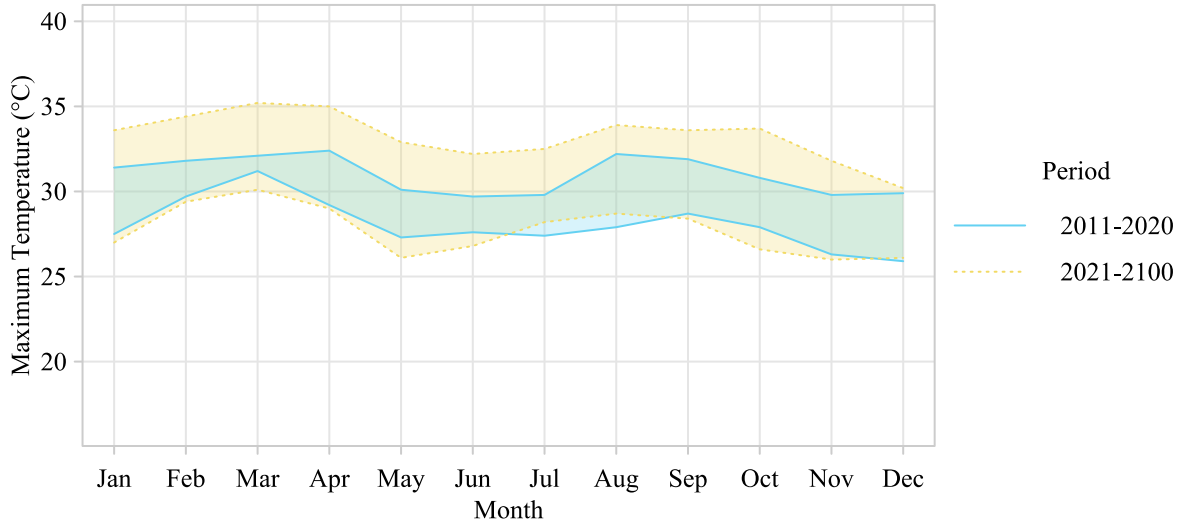


**Figure S4** Comparison of span of monthly maximum temperature outputs for seven CMIP6 models under SSP2/RCP4.5 during the periods 2011-2020 and 2021-2100.

*Additional Data*

Information on water quality, agronomic practices, and nutrient inputs was obtained for use in verifying the model and designing crop schedules. Sediment targets included an average annual soil yield of less than 10 tons/ha for the area of the watershed or less than 0.2 Mtons/year at the Sasumua Reservoir based on a study of the Tana River Basin (Hunink, et al., 2011).

A visit made to two progressive farms in the watershed provided experience used to further configure the model. A characterization of the two farms follows:

The operation of Farm 1 was highly responsive to market conditions, and the farmer, relatively new to the agrarian lifestyle, was open to experimentation and suggestions for management practices. Crops on Farm 1 included maize, Irish potato, kale, tree tomato, cabbage, and strawberry; livestock kept were rabbits and a dairy goat (Fig. S5a). Water features on Farm 1 included a sprinkler irrigation system for the strawberry plot fed from a plastic-lined runoff collection pond surrounded by a windbreak of maize and tall grass; this runoff collection pond with an approximated 50-$m^3$ capacity was established to provide a source of agricultural water during dry periods. The primary nutrient input was manure.

Farm 2 was under the management of a member of the Sasumua Water Resources Users Association (WRUA) and had a more structured approach to farming. Operation primarily followed the recommendations of the local extension service. Crops on Farm 2 included Irish potatoes, cabbage, kale, pear, and maize (Fig. S5b); livestock kept were chickens. Primary inputs for Farm 2 included manure, DAP, and potash. Two collection ponds of ~3.4 $m^3$ capacity, similar in construction to the pond described for Farm 1, were located throughout the property to store agricultural water. Farm 2 also had an additional natural pond in which water collects during the rainy season.


**Figure S5** Collections of photos featuring crops, livestock, conservation practices, and agricultural water harvesting systems found on location within the Sasumua River Watershed at (a) Farm 1 and (b) Farm 2.

Based on a countywide report, Irish potatoes, maize, garden peas, and cabbage are the primary crops grown in the region (County Government of Nyandarua, 2018). Seventy-seven percent of Nyandarua County households practice crop farming while 65% practice some form of animal husbandry (County Government of Nyandarua, 2018). Manure produced on the farm is applied to cropland and sometimes supplemented with purchased manure (Kimani et al., 2000, as cited in Kathuku et al., 2011; Odero, 1997); but little data is available on rates and composition of the application. Studies of other Kenyan regions indicate that the ranges of both are irregular, with most manure coming from cattle (Kimani et al., 2000, as cited in Kathuku et al., 2011; Lekasi et al., 2001). Inorganic fertilizer was used in 93% of farms in the greater Central Highlands region in 2004 with a rising trend (Ariga et al., 2006) and in 95% of potato farms studied more recently in Nyandarua (Mugo et al., 2020). Without field-specific data, a general uniform management schedule for agricultural land use was developed under the conditions of 100% participation in average manure application of 1700 kg/ha (Survey Area 114, Jaetzold et al., 2006). The fertilizer application rates summarized for the year 2012 in Oseko & Dienya (2015) as a weighted average for a crop distribution of 45% Irish potato, 20%

maize, 20% garden peas, and 15% cabbage were used (Table S5). There was similar fertilization rate data for 2013, however notes in the resource indicated that the 2013 growing year was irregular (Oseko & Dienya, 2015). The crop distribution approximation was based on the relative land cover area considering only the four widest spread crops in the county (County Government of Nyandarua, 2018) and rounded to the nearest 5%. Scheduling for the generic crop was roughly based on upper highlands climate zone activity for Irish potatoes and maize (Jaetzold et al., 2006), with annual chemical inputs evenly distributed between the two short growing seasons and the manure split into a band and side-dressing application.

**Table S5** Schedule for generic crop operations applied to agricultural land in the Sasumua River Watershed, Kenya.

| Date | Activity | Type | Name | Quantity (kg/ha) |
|---|---|---|---|---|
| March 10 & July 10 | Planting | - | Agricultural (agrl) | - |
| | Fertilizer Application | Band | DAP (18:46:00) | 52.1 |
| | | | Mavuno (15:10:22)* | 1.9 |
| | | | NPK 23:23:00* | 1.1 |
| | | | TSP (00:46:00)* | 1.0 |
| | Manure Application | Band | Fresh Dairy (dairy_fr) | 425.0 |
| April 30 & August 30 | Fertilizer Application | Side-Dress | CAN (15.5:00:00) | 17.6 |
| | | | Urea | 1.1 |
| | | | Mavuno (15:10:22)* | 0.2 |
| | Manure Application | Side-Dress | Fresh Dairy (dairy_fr) | 425.0 |
| June 30 & October 30 | Harvest | Vegetables | Agricultural (agrl) | - |

*Mavuno, NPK 23:23:00, and TSP were added to the SWAT+ database with fertilizer fractions for mineral N 0.15, 0.23, and 0.00, respectively, and mineral P 0.044, 0.101, and 0.203, respectively.

**Model Development, Calibration, and Validation**

A model for the Sasumua River Watershed was set up in QGIS 3.16.16 for SWAT+ Revision 60.5.2 using the developed data projected to ESRI:102022 - Africa Albers Equal Area Conic (Fig. 1). A channel threshold and stream threshold of 1.1 and 11 $km^2$, respectively, were selected to accommodate the creation of the reservoir stream section with no contributory channels and allow the point sources used to model diversions within the watershed to be positioned on streams while remaining consistent with the default 1:10 area ratio. The coordinates of inlets and outlets used can be found in Figure 8 in the main text and were based on field measurements, satellite imagery, and maps in literature (Dixon et al., 1958). One small subbasin closest to the main outlet, with an area of 0.17 $km^2$, was merged with the neighboring subbasin to its north. Slope percent bands were set at [0, 11, 22, 36, 57, 9999] based on natural breaks in the DEM histogram. Due to the difficulty of distinguishing between agricultural areas under specific crops or used as grazing land for livestock, the agricultural landuse was left as "Agricultural land generic" (AGRL) and not split. The landuse, soil, and slope thresholds for creation of Hydrologic Response Units (HRUs) were set to 0% to achieve a maximum level of detail. This yielded a model with 8 subbasins and 1,167 HRUs. Daily data on flowrates for the Kiburu or Chania diversions were not available, therefore, these features were modelled as a 90% diversion of flow from the channel at the diversion entrance to the exit point. This was achieved by first defining the inlet and outlet locations as point sources to break up the stream and increasing the number of outflows for the source channel, routing flow directly to the channel at the corresponding exit point.

The calibration period consisted of 2011-2015 with a 5-year warm up, and the validation period spanned 2016-2020. The calibration process order generally followed that of the original SWAT calibration procedure (Arnold et al., 2012), with a goal of achieving annual average water balance components within 15% of the target values and then proceeding with sediment calibration. Documentation for the automatic SWAT+ soft calibration procedure and work from preexisting studies of the watershed (Nduhiu et al., 2016; Mwangi et al., 2015) and the surrounding basin (Hunink et al., 2013) was referenced as a starting point for calibration parameters. A local sensitivity analysis was conducted for soft calibration of water balance proportions by observing the changes in SR and ET in response a ±5% change in the default values indicated in Table S6.

**Table S6** SWAT model parameters varied throughout initial sensitivity analysis and calibration runs.

| Parameter | Description | Unit | Default Value(s) | Possible Range | Testing Range | Change Type[1] | Calibrated Value |
|---|---|---|---|---|---|---|---|
| esco | Soil evaporation compensation factor | - | 0.95 | 0–1 | Sensitivity (0,1)<br>Calibration (0.64–0.68) | absval | 0.68 |
| epco | Plant uptake compensation factor | - | 1 | 0–1 | Sensitivity (0,1)<br>Calibration (0.98–1) | absval | 1 |
| petco | Hydraulic conductivity, K, of lowest layer | Fraction | ~0.00230 | 0.00161–0.00299 | Sensitivity (-20,20) | pctchg | -16.17 |
| cn3_swf | Soil water factor for cn3 0=fc; 1=saturation (porosity) | - | 0.95 | 0–1 | Sensitivity (0,1)<br>Calibration (0.98–1) | absval | 1 |
| latq_co | Plant evapotranspiration curve number coefficient | - | 0.01 | 0–1 | Sensitivity (0,1)<br>Calibration (0.40–0.48) | absval | 0.48 |
| flo_min | Minimum aquifer storage to allow return flow | m | 3 | 0–10 | Sensitivity (0,10) | absval | 8.10 |
| cn2 | Condition II curve number | - | CN~69-90 | 35–95 | Sensitivity (-25,5)<br>Calibration (-12– -8) | abschg | -12 |
| abf_lte | Alpha factor of groundwater | 1/days | 0.05 | 0–1 | Sensitivity (0,1) | absval | 0.49 |

[1]Change Type: absval - parameters were assigned the exact values indicated; abschg - parameter default value(s) were modified by the numbers indicated; pctchg - parameter default value was modified by the percentages indicated.

The analysis indicated that SR and ET were less sensitive to the parameters petco, flo_min, and abf_lte. However, preliminary runs suggested that the sensitivity of variables was highly dependent upon the parameter values chosen as a reference point. To explore the global parameter space further, the sensobol package in R was used to define a semi-random sample of parameter values mapped to uniform distributions over the ranges indicated in Table S6 and conduct a Saltelli first-order and Jansen total-order sensitivity analysis (Puy et al., 2021). The sample size n=500 for eight parameters corresponded to N=5,000 (4,953 unique) evaluations in SWAT+. Plots of the model output space for SR and ET versus the model input space suggested that, along the ranges tested, SR was most sensitive to cn3_swf and epco over the lower half of the range, and that ET was most sensitive to cn3_swf and

latq_co (Fig. S6). This was supported by the sensitivity analysis results which also indicated important interaction effects for these variables as well as esco and cn2 (Table S7), although sensitivities did not converge for all parameters given the small sample size.

The target composition values for SR and ET were 14% and 75% of annual rainfall for the calibration period, respectively, based on the corresponding ranges of 12-16% and 65-90% calculated and modelled in studies by Archer (1996), Hunink, et al. (2011), and Mwangi, et al. (2015). To select a combination of parameter values as a starting point for calibration, a filter was placed which excluded combinations exceeding 14±2.1% mean annual percent composition for SR. The highest mean percentage of ET achieved over the calibration period in the entire testing space was 44.1%, so the combination within the filtered space yielding the highest ET was selected. The parameters with total- or first-order sensitivity indices greater than 0.05 were adjusted slightly, but mean annual percentage ET could not be raised substantially without raising mean annual percentage SR beyond the desired range.

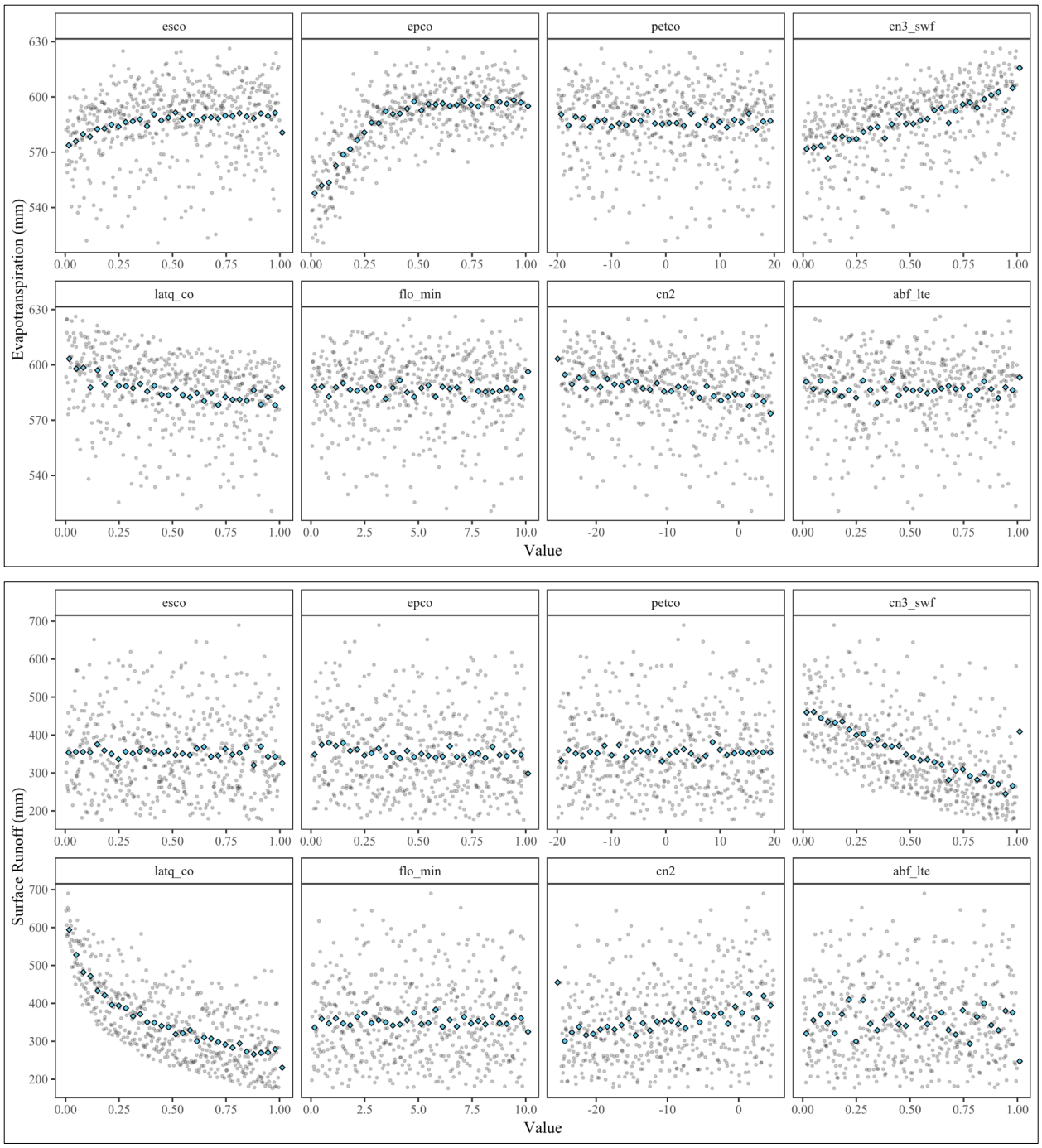


**Figure S6** Sensitivity analysis: plots of evapotranspiration and surface runoff output spaces for each parameter. Blue diamonds represent bin means.

**Table S7** Sensitivity analysis: indices of Saltelli first-order ($S_i$) and Jansen total-order ($T_i$) sensitivity for mean surface runoff and evapotranspiration results over the 2016-2020 calibration period.

| | | **Evapotranspiration** | | **Surface Runoff** | |
|---|---|---|---|---|---|
| **Parameter** | **Description** | **$S_i$** | **$T_i$** | **$S_i$** | **$T_i$** |
| esco | Soil evaporation compensation factor | 0.036 | 0.058 | 0.002 | 0.001 |
| epco | Plant uptake compensation factor | 0.510 | 0.596 | 0.009 | 0.008 |
| petco | Hydraulic conductivity, K, of lowest layer | 0.000 | 0.000 | 0.000 | 0.000 |
| cn3_swf | Soil water factor for cn3 0=fc; 1=saturation | 0.235 | 0.252 | 0.341 | 0.370 |
| latq_co | Plant evapotranspiration curve number coefficient | 0.076 | 0.082 | 0.601 | 0.593 |
| flo_min | Minimum aquifer storage to allow return flow | 0.000 | 0.000 | 0.000 | 0.000 |
| cn2 | Condition II curve number | 0.017 | 0.046 | 0.048 | 0.070 |
| abf_lte | Alpha factor of groundwater | 0.000 | 0.000 | 0.000 | 0.000 |

Footnote: $S_i$ represents the first-order effect, the fractional contribution of the parameter to model uncertainty; $T_i$ represents the total-order effect, the joint measurement of the first-order effect and all other parameters in the analysis. Indices greater than 0.05 were considered an implication of parameter significance.

**References**


Archer, D. (1996) Suspended sediment yields in the Nairobi area of Kenya and environmental controls. In Erosion and sediment yield: global and regional perspectives. Proceedings of the Exeter Symposium, July 1996, Eds. Walling, D.E. & Webb, B.W. Vol. 236, 37–48.

Ariga, J., Jayne, T.S., & Nyoro, J. (2006) Factors Driving the Growth in Fertilizer Consumption in Kenya, 1990-2005: Sustaining the Momentum in Kenya and Lessons for Broader Replicability in Sub-Saharan Africa. Tegemeo Working paper 24/2006. https://citeseerx.ist.psu.edu/viewdoc/download?doi=10.1.1.188.1519&rep=rep1&type=pdf Accessed 5 March 2022.

Arnold, J. G., Moriasi, D. N., Kannan, N., Jha, M. K., Gassman, P. W., Abbaspour, K. C., White, M. J., Srinivasan, R., Santhi, C., Harmel, R. D., Griensven, A. V., & Van Liew, M. W. (2012). SWAT: Model Use, Calibration, and Validation. *Transactions of the ASABE*, 55(4), 1491–1508. https://doi.org/10.13031/2013.42256

Arnold, J. G., Kiniry, J. R., Srinivasan, R., Williams, J. R., Haney, E. B., & Neitsch, S. L. (2013). SWAT 2012 input/output documentation. Texas Water Resources Institute, TR-439. https://swat.tamu.edu/media/69296/swat-io-documentation-2012.pdf

County Government of Nyandarua. (2018) Nyandarua County Integrated Development Plan (CIDP2) 2018-2022. https://repository.kippra.or.ke/handle/123456789/663. Accessed 15 March 2022.

Dijkshoorn J.A., Macharia P.N., Huting J.R.M., Maingi P.M. & Njoroge C.R.K. (2011). Soil and terrain conditions for the Upper Tana River catchment, Kenya. (ver1.1). Green Water Credits Report 11 / ISRIC Report 2010/09b, ISRIC – World Soil Information, Wageningen. https://isric.org/sites/default/files/isric_report_2010_09b.pdf

Dixon, H. H., Edington, G., & Fitzgerald, E. (1958). The Chania-Sasumua Water Supply for Nairobi. *Proceedings - Institution of Civil Engineers*, *9*(4), 345–368. https://doi.org/10.1680/iicep.1958.2302

Garibay, V. M., Gitau, M. W., Kiggundu, N., Kisekka, J., Kongo, V., Mati, B., Moriasi, D., Munishi, S. E. (2022). Precipitation and Temperature Data from 10 CMIP6 Models for Sasumua River Watershed, Kenya. Purdue University Research Repository. https://doi.org/10.4231/DATG-PB58

Garibay, V. M., Gitau, M. W., Kiggundu, N., Moriasi, D., & Mishili, F. (2021). Evaluation of Reanalysis Precipitation Data and Potential Bias Correction Methods for Use in Data-Scarce Areas. *Water Resources Management*, 35(5), 1587–1602. https://doi.org/10.1007/s11269-021-02804-8

Hengl T., Mendes de Jesus J., Heuvelink G.B.M., Ruiperez Gonzalez M., Kilibarda M., Blagotić A., Shangguan, W., Wright, M.N., Geng, X., Bauer-Marschallinger, B. & Guevara, M.A. (2017) SoilGrids250m: Global gridded soil information based on machine learning. *PLoS ONE*, 12(2), e0169748. https://doi.org/10.1371/journal.pone.0169748

Hunink, J. E., & Droogers, P. (2011). Physiographical baseline survey for the Upper Tana catchment: erosion and sediment yield assessment. *Future Water Report*, 112, 31. https://futurewater.nl/wp-content/uploads/2013/01/2011_TanaSed_FW-1121.pdf Accessed 7 Jan 2022.

Hunink, J. E., Niadas, I. A., Antonaropoulos, P., Droogers, P., & De Vente, J. (2013). Targeting of intervention areas to reduce reservoir sedimentation in the Tana catchment (Kenya) using SWAT. *Hydrological Sciences Journal*, 58(3), 600–614. https://www.isric.org/sites/default/files/isric_gwc_report_k10.pdf Accessed 17 February 2022.

Hong, S.Y., Minasny, B., Han, K.H., Kim, Y., & Lee, K. (2013). Predicting and mapping soil available water capacity in Korea. PeerJ 1:e71 https://doi.org/10.7717/peerj.71

Jaetzold, R., Schmidt, H., Hornetz, B., & Shisanya, C. (2006). Farm management handbook of Kenya: Volume II: Natural conditions and farm management information; Part B: Central Kenya; Subpart B2: Central Province (2nd ed.). Kenya Ministry of Agriculture. https://star-www.giz.de/fetch/88Xl00jdWg0001Q1JV/07-1284.pdf Accessed 24 March 2022.

Kathuku, A., Kimani, S., Okalebo, J., Othieno, C., & Vanlauwe, B. (2011) The Effects of Integration of Organic and Inorganic Sources of Nutrient on Maize Yield in Central Kenya. In: Bationo, A., Waswa, B., Okeyo, J., Maina, F., Kihara, J. (eds) *Innovations as Key to the Green Revolution in Africa*. Springer, Dordrecht. https://doi.org /10.1007/978-90-481-2543-2_25

Lekasi, J.K., Tanner, J.C., Kimani, S.K. & Harris, P.J.C. (2001). *Managing Manure to Sustain Smallholder Livelihoods in the East African Highlands*. HDRA, Ryton-on-Dunsmore. ISBN 0 905343

Mockus, V., Werner, J., Woodward, D. E., Nielsen, R., Dobos, R., Hjelmfelt, A., & CC, H. (2009). Part 630 Hydrology National Engineering Handbook: Chapter 7: Hydrologic soil groups. US Department of Agriculture: Natural Resources Conservation Service. https://directives.sc.egov.usda.gov/OpenNonWebContent.aspx?content=17757.wba

Mugo, J. N., Karanja, N. N., Gachene, C. K., Dittert, K., Nyawade, S. O., & Schulte-Geldermann, E. (2020). Assessment of soil fertility and potato crop nutrient status in central and eastern highlands of Kenya. *Scientific Reports*, 10(1), 7779–7779. https://doi.org/10.1038/s41598-020-64036-x

Mwangi, J. K., Shisanya, C. A., Gathenya, J. M., Namirembe, S. & Moriasi, D. N. (2015) A modeling approach to evaluate the impact of conservation practices on water and sediment yield in Sasumua watershed, Kenya. *Journal of Soil and Water Conservation*, 70(2), 75–90. https://doi.org/10.2489/jswc.70.2.75

Nduhiu, C., Gathenya, J. M., Mwangi, J. K., Aman, M., & Mutisya, T. (2016). Assessment of the effectiveness of Payment for Ecosystem Services (PES) in the delivery of desired Ecosystem Services in Sasumua catchment, Kenya. *Hydrology and Earth System Sciences Discussions*, 1–20. https://doi.org/10.5194/hess-2016-541

Odero, K.K. (1997). The direct and indirect effects of road quality Improvement: a study of fertilizer use and Potato Yield in Kinangop division, Nyandarua District, Kenya. [Doctoral Thesis, University of Nairobi]

http://erepository.uonbi.ac.ke/bitstream/handle/11295/22404/Odero_The%20direct%20and%20indirect%20effects%20of%20road%20quality%20Improvement.pdf Accessed 26 April 2022.

O'Geen, A. T. (2013) Soil Water Dynamics. Nature Education Knowledge 4(5):9 https://www.nature.com/scitable/knowledge/library/soil-water-dynamics-103089121/

O'Neill, B. C., Tebaldi, C., van Vuuren, D. P., Eyring, V., Friedlingstein, P., Hurtt, G., Knutti, R., Kriegler, E., Lamarque, J.-F., Lowe, J., Meehl, G. A., Moss, R., Riahi, K., & Sanderson, B. M. (2016) The Scenario Model Intercomparison Project (ScenarioMIP) for CMIP6, *Geoscientific Model Development*, 9, 3461–3482, https://doi.org/10.5194/gmd-9-3461-2016.

Oseko, E. & Dienya, T. (2015). Fertilizer consumption and fertilizer use by crop (FUBC) in Kenya. https://africafertilizer.org/wp-content/uploads/2017/05/FUBC-Kenya-final-report-2015.pdf Accessed 26 April 2022.

Post, D. F., Fimbres, A., Matthias, A. D., Sano, E. E., Accioly, L., Batchily, A. K., & Ferreira, L. G. (2000). Predicting Soil Albedo from Soil Color and Spectral Reflectance Data. Soil Science Society of America Journal, 64(3), 1027–1034. https://doi.org/10.2136/sssaj2000.6431027x

Puy, A., Piano, S. L., Saltelli, A., & Levin, S. A. (2021). Sensobol: an R package to compute variance-based sensitivity indices. https://doi.org/10.48550/arXiv.2101.10103.

Riahi, K., van Vuuren, D. P., Kriegler, E., Edmonds, J., O'Neill, B. C., Fujimori, S., Bauer, N., Calvin, K., Dellink, R., Fricko, O., Lutz, W., Popp, A., Cuaresma, J., C., KC, S., Leimbach, M., Jiang, L., Kram, T., Rao, S., Emmerling, J., Ebi, K., Hasegawa, T., Havlik, P., Humpenoder, Fl., Da Silva, L. A., Smith, S., Stehfest, E., Bosetti, V., Eom, J., Gernaat, D., Masui, T., Rogelj, J., Strefler, J., Drouet, L., Krey, V., Luderer, G., Harmsen, M., Takahashi, K., Baumstark, L., Doelman, J. C., Kainuma, M., Klimont, Z., Marangoni, G., Lotze-Campen, H., Obersteiner, M., Tabeau, A., & Tavoni, M. (2016). The Shared Socioeconomic Pathways and their energy, land use, and greenhouse gas emissions implications: An overview. *Global Environmental Change*, 42, 153–168. https://doi.org/10.1016/j.gloenvcha.2016.05.009

Saha, S., Moorthi, S., Pan, H., Wu, X., Wang, J., Nadiga, S., Tripp, P., Kistler, R., Woollen, J., Behringer, D., Liu, H., Stokes, D., Grumbine, R., Gayno, G., Wang, J., Hou, Y., Chuang, H., Juang, H. H., Sela, J., Iredell, M., Treadon, R., Kleist, D., Van Delst, P., Keyser, D., Derber, J., Ek, M., Meng, J., Wei, H., Yang, R., Lord, S., van den Dool, H., Kumar, A., Wang, W., Long, C., Chelliah, M., Xue, Y., Huang, B., Schemm, J., Ebisuzaki, W., Lin, R., Xie, P., Chen, M., Zhou, S., Higgins, W., Zou, C., Liu, Q., Chen, Y., Han, Y., Cucurull, L., Reynolds, R. W., Rutledge, G., & Goldberg, M. (2010). NCEP Climate Forecast System Reanalysis (CFSR) 6-hourly Products, January 1979 to December 2010. Research Data Archive at the National Center for Atmospheric Research, Computational and Information Systems Laboratory. https://doi.org/10.5065/D69K487J.

Saha, S., Moorthi, S., Wu, X., Wang, J., Nadiga, S., Tripp, P., Behringer, D., Hou, Y., Chuang, H., Iredell, M., Ek, M., Meng, J., Yang, R., Mendez, M. P., van den Dool, H., Zhang, Q., Wang, W., Chen, M., & Becker, E. (2011, updated daily). NCEP Climate Forecast System Version 2 (CFSv2) 6-hourly Products. Research Data Archive at the National Center for Atmospheric Research, Computational and Information Systems Laboratory. https://doi.org/10.5065/D61C1TXF.

Saxton, K. E., & Rawls, W. J. (2006). Soil Water Characteristic Estimates by Texture and Organic Matter for Hydrologic Solutions. Soil Science Society of America Journal, 70(5):1569-1578. https://www.proquest.com/scholarly-journals/soil-water-characteristic-estimates-texture/docview/216075311/se-2?accountid=13360

Saxton, K.E., Rawls, W.J., Romberger, J.S. & Papendick, R.I. (1986). Estimating generalized soil-water characteristics from texture. Soil Science Society of America Journal. 50(4):1031-1036. https://doi.org/sssaj1986.03615995005000040039x

Van Engelen, V. W. P., & Dijkshoorn, J. A. (2012). Global and National Soils and Terrain Databases (SOTER). Procedures Manual, version 2.0, draft for comments. ISRIC Report 2012/04, ISRIC–World Soil Information, Wageningen. ISRIC Report

# APPENDIX II: CASE STUDY RESULTS SUPPLEMENT

Monthly and seasonal flow results of SSP2/RCP4.5 were plotted to provide a more detailed snapshot of projected changes (Fig. S7). The greatest monthly increases between the first and final periods are present in November through January, a feasible response to the rise in short rains precipitation maximums (Fig. S2); seasons show a steady increase over time with the exception of the second dry season (June-August), which exhibits little change.

Subbasin-level differences in surface runoff (SR) and evapotranspiration (ET) were mapped for each considered period (Fig. S8 & S9). Both SR and ET increase for all subbasins between the first and fourth periods. Modelled results for SR are more stratified across the watershed throughout the periods and amounts rise substantially over time. Results for the northernmost subbasin, already susceptible to the greatest sediment losses, show an increase from 1.4 (baseline) to 2.2 (2071-2090) times the area-weighted mean for baseline SR.

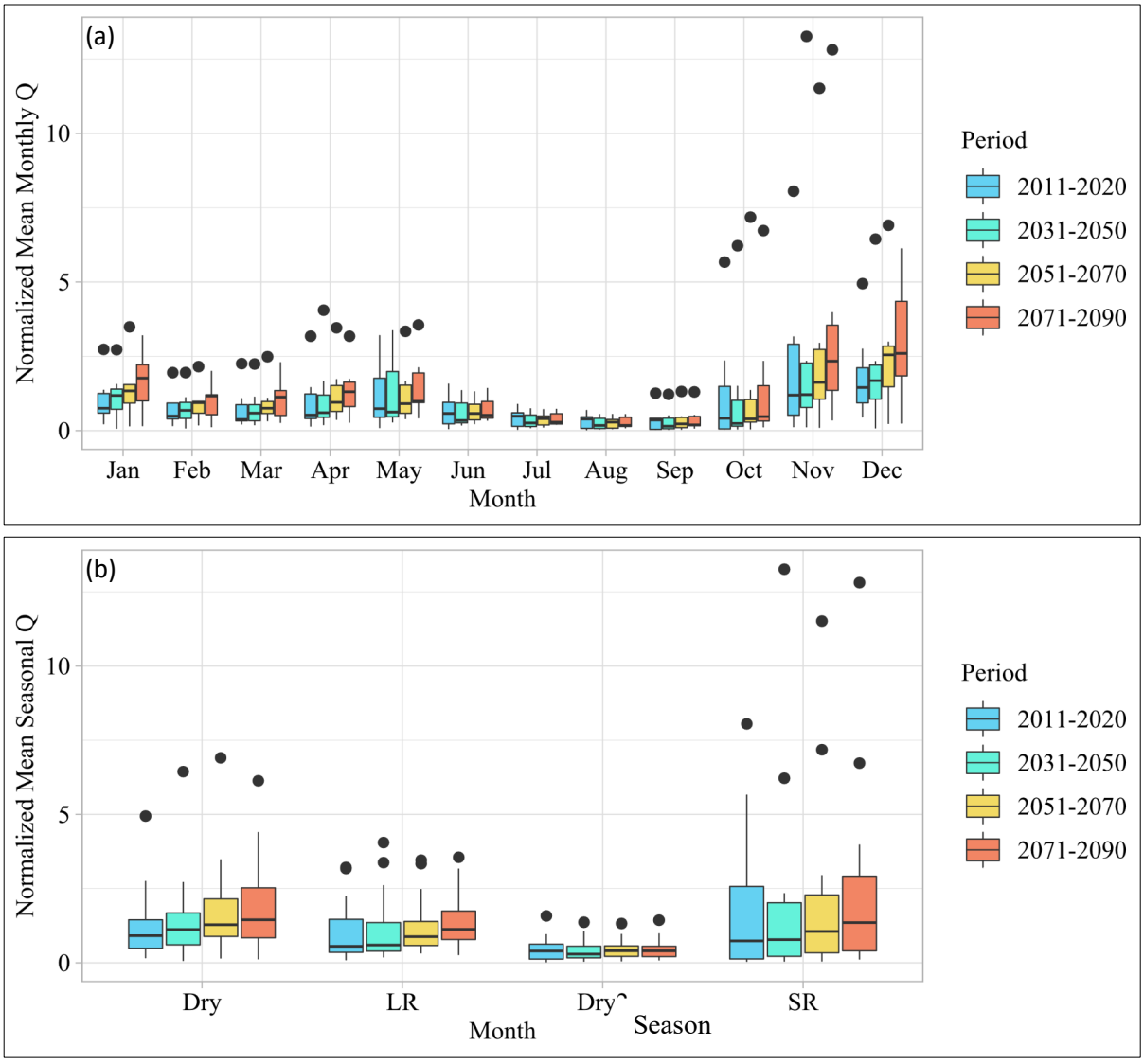


**Figure S7** Boxplots for (a) mean monthly discharge and (b) mean seasonal discharge into the Sasumua Reservoir for the periods 2011-2020 (baseline), 2031-2050, 2051-2070, and 2071-2090 under SSP2/RCP4.5 using outputs from seven CMIP6 models. Average monthly flows were normalized using the median monthly value for the first period. Average seasonal flows were normalized using the median value for the first dry season of the first period. Points represent statistical outliers and are not considered in the formation of the boxplots.

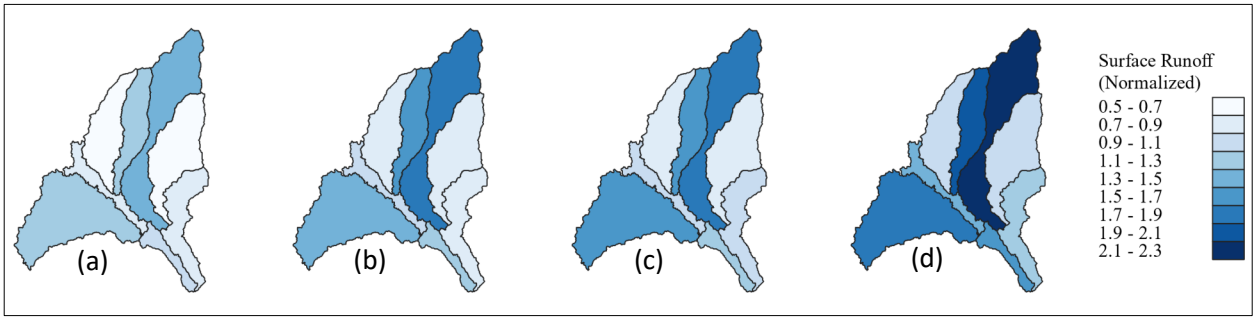


**Figure S8** Mean annual surface runoff by subbasin for (a) 2011-2020 (baseline), (b) 2031-2050, (c) 2051-2070, and (d) 2071-2090 using outputs from seven CMIP6 models. Values normalized on basis of area-weighted mean for 2011-2020 period.

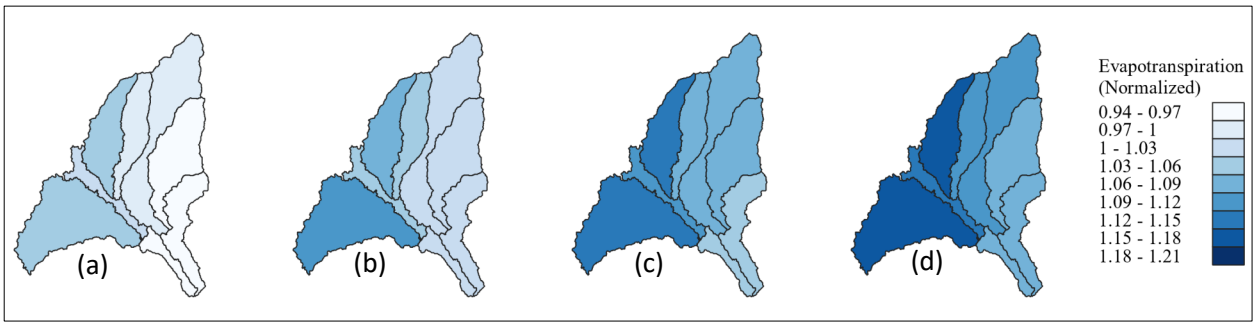


**Figure S9** Mean annual evapotranspiration by subbasin for (a) 2011-2020 (baseline), (b) 2031-2050, (c) 2051-2070, and (d) 2071-2090 using outputs from seven CMIP6 models. Values normalized on the basis of the area-weighted mean for the 2011-2020 period.

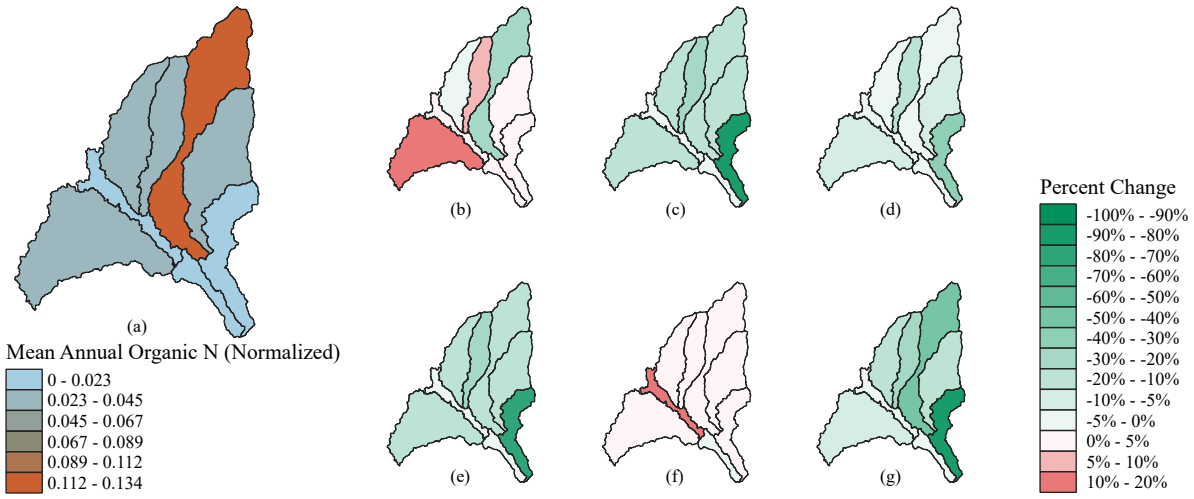


**Figure S9** Map of organic nitrogen loss by subbasin for: a) baseline; and scenarios b) 1-Riparian Buffers, c) 2-Filter Strips, d) 3-Terracing, e) 4-Field Diversions, f) 5-Agricultural Water Harvesting Ponds, and g) 6-Combined Application of 1, 2, 3, and 5. All scenario percent changes are relative to baseline. Reductions in losses are signified by a negative percent change. Baseline values normalized on basis of area weighted mean for entire basin.

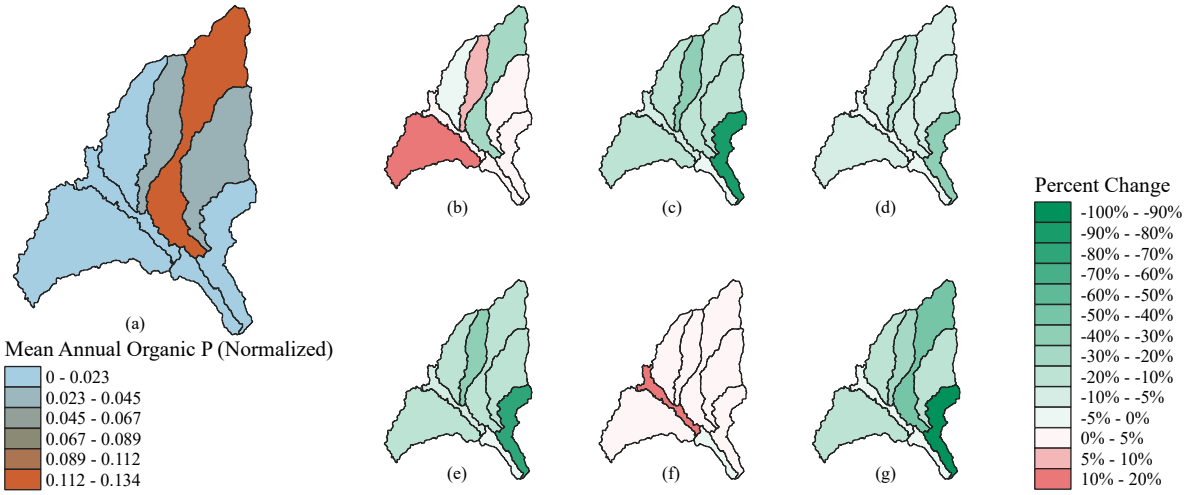


**Figure S10** Map of organic phosphorous loss by subbasin for: a) baseline; and scenarios b) 1-Riparian Buffers, c) 2-Filter Strips, d) 3-Terracing, e) 4-Field Diversions, f) 5-Agricultural Water Harvesting Ponds, and g) 6-Combined Application of 1, 2, 3, and 5. All scenario percent changes are relative to baseline. Reductions in losses are signified by a negative percent change. Baseline values normalized on basis of area weighted mean for entire basin.